University of Washington

Abnormal Gait Detection using Wearable Hall-Effect Sensors

Courtney Chan Chheng

A thesis

submitted in partial fulfillment of the

requirements for the degree of

Master of Science in Electrical Engineering

University of Washington

2021

Committee:

Denise Wilson

Seungkeun Choi

Kaibao Nie

Program Authorized to Offer Degree:

Electrical Engineering

University of Washington

University of Washington

Abstract

Abnormal Gait Detection using Wearable Hall-Effect Sensors

Courtney Chan Chheng

Chair of the Supervisory Committee: Denise Wilson
Department of Electrical Engineering

Abnormalities and irregularities in walking (gait) are predictors and indicators of both disease and injury. Gait has traditionally been monitored and analyzed in clinical settings using complex video (camera-based) systems, pressure mats, or a combination thereof. This thesis presents an alternative, wearable gait monitoring system designed to be worn on the inner knee or upper thigh that consists of low-power Hall-effect sensors positioned on one leg and a compact magnet positioned on the opposite leg. Wireless data collected from the sensor system were used to analyze stride width, stride width variability, cadence, and cadence variability for four different individuals engaged in normal gait, two types of abnormal gait, and two types of irregular gait. Using leg gap variability as a proxy for stride width variability, 81% of abnormal or irregular strides were accurately identified as different from normal stride. Cadence was surprisingly 100% accurate in identifying strides which strayed from normal, but variability in cadence provided no useful information. This highly sensitive, non-contact Hall-effect sensing method for gait monitoring offers the possibility for detecting visually imperceptible gait variability in natural settings. These nuanced changes in gait are valuable for predicting early stages of disease and also for indicating progress in recovering from injury.

TABLE OF CONTENTS

LIST OF FIGURES

LIST OF TABLES

ACKNOWLEDGEMENT & DEDICATION

I would like to sincerely thank Professor Denise Wilson, whom has been not only a close research advisor but a mentor to me for many years. Without her careful guidance, I would have never been able to pursue this thesis and research for all these years. Professor Wilson is an incredible educator and person, with the utmost care for her students, of which I will never forget. Despite my short-comings, Professor Wilson always came knocking on my door to bring me back to my goals, and for that I have the deepest gratitude to her.

I would also like to thank Professor Seungkeun Choi for his support and mentorship throughout this research. It is not without his encouragement and dedication to my education that this thesis was completed.

I would also like to thank Professor Kaibao Nie, for his time and guidance towards this thesis.

Finally, I would also like to thank E. Parry, and A. Thai of the Department of Electrical Engineering, University of Washington, for their technical assistance in the preliminary work associated with this project.

This research is dedicated to my mother and father, Narine and Thai Chheng. Thank you for supporting and loving me for all my years. And to my husband-to-be, Logan Stimson, thank you for everything from the bottom of my heart.

Chapter 1

INTRODUCTION

How individuals walk (i.e., gait) can vary as a result of walking surface, individual body type, injury, disease, fatigue, and a variety of other factors. Abnormalities or irregularities in gait can both predict and indicate health problems. However, monitoring gait for these abnormalities or irregularities currently requires a significant capital investment.

1.1. Terminology: Gait Parameters

For an activity as complex as human locomotion, it might seem obvious that there are a wide variety of nuances to gait that require monitoring. To capture the complexity of gait, a wide range of parameters are used. Figure 1.1 illustrates several of these gait parameters, including step length, stride length, stride width, and midstance, in proportion to leg gap.

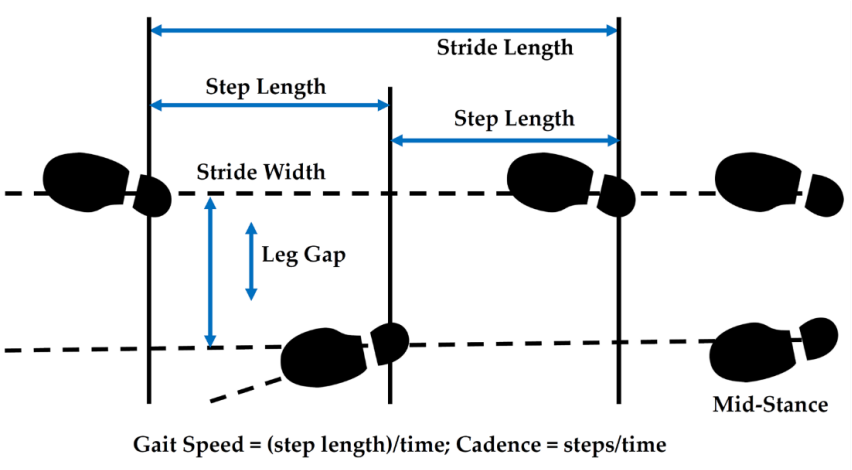

Figure 1.1. Gait Parameters.

Figure graphically illustrates several gait parameters measured in gait. This research will focus on that of stride width and cadence.

A stride is simply a sequence of two steps. Stride width is the distance between two imaginary parallel lines, passing through the heel of the foot [1] during a stride. Variability in stride width is typically described in terms of the coefficient of variation (i.e., standard deviation divided by the mean) or standard deviation in stride width for a group of similar strides [2]. It is noteworthy that in many scenarios,

cadence serves as a context for studying other gait parameters. Knowing cadence allows variations in other gait parameters to be assessed more accurately.

There is significant literature to exemplify that abnormalities or irregularities in gait can predict and indicate health problems. Disturbances in gait have been found to be linked to a variety of diseases, disorders, physical and neurological impairments and recovery and rehabilitation, discussed next.

1.2 Neurological Disease and Disorders

Neurological diseases and disorders often affect how an individual walks, often in ways that are characteristics of the neurological malfunction (Table 1.1). Sometimes, these gait issues can be characterized in terms of specific gait parameters. For example, variability in stride width has been found to be the most reliable gait variable in assessing gait variability in patients with Parkinson's disease [3]. In contrast, studies of individuals with Parkinson's disease have demonstrated no significant differences in cadence from typically developed (healthy) adults [4]. Parkinson's Disease has been the subject of many studies relating to the study of gait parameters. Gait irregularities such as freezing of gait [5]–[10], or interrupted cadence, and bradykinesia (slowness of movement) are known as cardinal symptoms of Parkinson's Disease and measurement of these parameters are used in diagnosis of the disease. Studies have also shown that increased stride width variability [5], [7], [11], shortened stride length [5]–[7], [10], increased stride time [7], slowed movement [7], [9], increased variability of double support timing [7], increased variability of gait cycle duration [7], increased stride to stride variability [7], and difficulty crossing a threshold [10] are just an example of some of the parameters that may be utilized in the diagnosis and treatment of Parkinson's disease.

Alzheimer's disease is another example of a disease that could benefit from the further study of gait parameters. Parameters such as increased stance time [12], decreased step length [11], [12], reduced cadence [12], [13], increased stride length variability [13], stride time variability [13], can also be used in the diagnosis and treatment of Alzheimer's disease. In addition to Parkinson's disease and Alzheimer's disease, among children with cerebral palsy, gait is monitored to guide and improve the viability of

adapted walking strategies during rehabilitation training in children [14]. Lastly, Huntington's disease, similar to the gait parameters of Parkinson's disease, can be characterized by gait abnormalities such as increased stride to stride variability [7], [15], slowed movement [15], decreased gait stability [7], increased cadence variability [7], and increased stride to stride variability [7].

Table 1.1. Gait Issues associated with Neurological Disease & Disorder

	Gait Abnormality/Irregularity	**Ref**
Parkinson's Disease	Freezing of Gait (Interrupted Cadence)	[5]–[10]
	Increased Stride Width Variability	[5], [7], [11]
	Shorter Stride Length	[5]–[7], [10]
	Increased stride time	[7]
	slowed movement	[7], [9]
	Increased variability of double support timing	[7]
	Increased variability of gait cycle duration	[7]
	Increased stride to stride variability	[7]
	Difficulty crossing a threshold	[10]
Alzheimer's Disease	Increased Stance Times	[12]
	Decreased step length	[11], [12]
	Reduced Cadence	[12], [13]
	Increased stride length variability	[13]
	Stride time variability	[13]
Cerebral Palsy	Stride to Stride variability	[14]
Huntington's Disease	Increased stride to stride variability	[7], [15]
	slowed movement	[15]
	Decreased gait stability	[7]
	Increased cadence variability	[7]
	Increased stride to stride variability	[7]
Multiple Sclerosis	Slower cadence	[16]
	Limited range of motion	[16]
	Reduced Stability	[16]

1.3 Mental Health Disorders

Measurement of gait parameters could also aid in the diagnosis or treatment of mental health disorders (Table 1.2). Included in these mental health disorders is depression. According to the American Psychiatric Association, depression affects an estimated one in fifteen adults in any given year, and even worse yet, one in six people will experience depression at some time in their life and is the leading cause of disability for ages 15 to 44. As such, depression is an important mental health issue that society cannot ignore. However, monitoring of gait disturbances can aid in the diagnosis or treatment of these disease. For instance, depressed persons often walk more slowly [17]. In addition to lowered velocity, depressed persons have shown reduced stride length [17], increased double limb support [17], and decreased cadence [6], [18]. Similarly, bipolar disordered persons have shown decreased cadence [18], shortened swing phase time [18], and swing time variability [18].

Table 1.2. Gait Issues associated with Mental Health Disorders

	Gait Abnormality/Irregularity	**Ref**
Depression	Lower gait velocity	[17]
	Reduced stride length	[17]
	Increased double limb support	[17]
	Increased Cycle duration	[17]
	Decreased cadence	[6], [18]
	Decreased swing phase time	[18]
Bipolar Disorder	Swing time variability	[18]
	Decreased Cadence	[18]
	Shortened swing phase time	[18]

1.4 Physical and Neurological Impairments

Disturbances in gait have been found to be early predictors of physical and neurological impairments (Table 1.3). Among physical impairments, loss of vision has been associated with decreased walking speed, among other factors [19]. According to the CDC, in the United States, over 12 million Americans aged 40 and over have some sort of vision impairment, including one million of which are blind [20]. According to the United Nations, by 2050, one in six people in the world will be over the age of 65, a

number that is up from one in 11 in 2019. As the general population of the world increase, the number of people with age-related cognitive impairment is also expected to increase. As such, it is also important to better understand how to diagnose and treat these conditions. Age-related cognitive impairment has been associated with the gait parameters of increased stride variability, and decreased cadence.

Table 1.3. Gait Issues associated with Physical and Neurological Impairment

	Gait Abnormality/Irregularity	**Ref**
Loss of Vision	Decreased cadence	[19]
	Increase in center of mass up termination of walking	[19]
Age-Related Cognitive Impairment	Increased stride variability	[21]
	Decreased cadence	[21]
Peripheral Neuropathy	Increased step time variability	[19]

1.5 Injury and Risk of Injury

In addition, injuries and risk of injuries can be linked to abnormality or irregularly (Table 1.4). Among these include that of fall risk in the elderly and of physical disability [2], [22]. Falls are an important health concern and can result in serious injuries, enduring disabilities, and drastic life-style changes [23]. Therefore, estimation of fall risk among the vulnerable and elderly should be of high priority to the aging population. Fall risk has been identified to be measured by the following measurable gait parameters: increased stride time variability [22], lowered balance [19], wider stance [24], decreased cadence [16], [23]–[25], decreased stride length [23], double-support time variability [24], stride length variability [24], limited range of motion [16], and increased variability in spatiotemporal gait characteristics [16]. In addition to fall risk among the elderly, runners at risk for tibial stress fractures have also been linked to gait irregularity. These runners have shown increase in cadence [26].

Table 1.4. Gait Issues associated with Injury and Risk of Injury

	Gait Abnormality/Irregularity	**Ref**
Tibia Fractures	Increased cadence	[22]
Fall Risk	Increase stride time variability	[22]
	Lowered balance	[19]
	Wider stance	[24]
	Decreased cadence	[16], [23]–[25]
	Decrease stride length	[23]
	Double-support time variability	[24]
	Swing time variability	[24]
	Stride length variability	[24]
	Limited range of motion	[16]
	Increased variability in spatiotemporal gait characteristics	[16]

1.6 Recovery and Rehabilitation

Gait also changes as individuals recover from injury or adapt to disability, and monitoring gait during these processes provides valuable information regarding the success or failure of rehabilitation strategies. Monitoring of gait parameters, such as cadence, can also support the prevention of injury. Patients recovering from knee replacement can benefit from the monitoring of stride parameters such as stride width, gravity center fluctuation and walking velocity [27].

Thus, monitoring the simple act of walking can provide important information for detecting, treating, and healing from injury, for early detection and diagnosis of disease, and for identifying risk of injury among the elderly and other vulnerable populations.

Table 1.5. Gait Issues associated with Recovery and Rehabilitation

	Gait Abnormality/Irregularity	**Ref**
Knee Replacement	Stride Width	[27]
	Gravity center fluctuation	[27]
	Walking velocity	[27]
Peripheral Neuropathy	Increased step time variability	[19]

1.7 Current technology in the Monitoring of Gait

Currently, monitoring of gait is contained to mostly a clinical setting. Current monitoring of gait is conducted in a clinical setting with camera monitoring systems that visually capture gait and are often combined with force platforms which capture ground reaction forces as an individual walk [29]. Access to clinical monitoring is limited as these specialized locomotion laboratories require significant capital investment and lengthy setup and post-processing time [9]. Moreover, clinical monitoring is limited only to controlled gait analysis, as patients often don't seek help until there is a known issue. In contrast, the use of wearables technology for monitoring of gait could expand access to gait monitoring, as wearables have the potential to expand and equalize access to quality health care across different populations.

Chapter 2

BACKGROUND

Human locomotion is complex and monitoring gait is a diverse problem that cannot be addressed with only a single approach. Gait itself requires several muscles, bones, and movements to enable locomotion of the body. It is thus no surprise that there is vast literature on the many different types of approaches to gait monitoring. Some methods are reserved for clinical settings, while others use wearables to aid in the monitoring of gait.

2.1 Clinical Monitoring Techniques

Because the normalness of gait is affected by a wide range of factors, not all of which involve disease or injury, a vast majority of gait irregularity studies have been restricted to clinical settings. In clinical settings, extraneous factors can be controlled in order to focus on detecting and assessing gait disturbances that stem from physical injury, psychological origins, or central nervous system disease. In the clinical setting, gait analysis is typically conducted with camera monitoring systems that visually capture gait and are often combined with force platforms which capture ground reaction forces on the feet as an individual walks. These multi-sensor, three-dimensional systems capture an immense amount of data that are typically evaluated off-site by a qualified physician or other medical professional [9]. Further, clinical gait monitoring equipment is often only found in gait or specialized locomotion laboratories and requires significant capital investment and lengthy setup and post-processing times [28]. In addition, these costly laboratories raise questions of access for the general population, as they may not be available in rural areas or to lower income individuals. And not only is access to clinical gait monitoring often limited, but it can require significant post-processing time. Data collected from these locomotion laboratories is often sent to a specialist for post-processing, where the analysis and diagnosis may take weeks to reach the patient. Thus, not only is clinical gait monitoring limited to only controlled gait analysis, but it is also likely that it is accessed only when patients have issues that have reached an extreme in gait health.

Moreover, since gait monitoring technologies in clinical settings are typically not worn on the body, they are vulnerable to interference from ambient conditions, incomplete data regarding the full range of gait, and data transfer and processing capability. Cameras capture human movement and then utilize video and image processing to extract gait parameters [29]. These systems have the advantage of accurately capturing many nuances of observable gait but are expensive and processing of image data is often hindered by variations in the spectrum and intensity of ambient illumination. Further, camera-based methods, especially those that capture gait in three-dimensions, generate large amounts of data which limit the opportunity to process the data in real time and create bandwidth and storage issues at the back end of these systems. As importantly, while camera-based systems provide prolific and accurate information about disturbances in gait, they are inherently limited in identifying the source of those disturbances. For example, an individual who is limping may be doing so to avoid pain for any number of reasons which remain largely opaque and inaccessible to camera-based systems. To address this lack of contact-based information, force-sensitive platforms are a common supplement or alternative to camera-based systems in clinical settings. The force-sensitive platform contains force sensors embedded in walking pads or platforms. Each pressure pad contains large arrays of pressure sensors placed in a grid array which are then interconnected with each other [29]. These platforms track in considerable detail the forces exerted by each foot as an individual walks and can provide not only accurate measures of step length, stride length, stride width, cadence, and similar parameters, but also monitor abnormalities in foot pressure that can be indicative of unhealthy posture, injury, or disease. While these high-resolution data are invaluable for providing greater insight into the forces on the feet and subsequent gait disturbances, they only monitor the feet when they are in contact with the floor (i.e., platform) and therefore lack information generated during the swing phase of gait [29], [30]. Wearable sensors, while providing less accurate and less complete data regarding gait, can fill some of the present gaps left by clinical gait monitoring.

2.2. Wearable Technology

A viable alternative to clinical gait monitoring is to explore the value and future of using wearable technology to monitor gait. Wearable sensor systems support a more practical health care paradigm which not only expands access but also equalizes access to care across different populations. Systems that can deliver health care services at any time and to any location have significant global implications for supporting personalized health care, disease prevention, point-of-care diagnosis, and treatment of chronic disease conditions [31], [32]. Wearable sensor systems also open new possibilities for continuous monitoring, timely decision making, and reductions in unnecessary hospitalization while also being non-invasive or minimally invasive to their subjects [31], [33]. Moreover, in contrast to clinical monitoring, wearable sensors have the unique and valuable advantage of monitoring subjects in their natural setting. Especially relevant to gait monitoring, wearable sensors can drive down the health care costs of an aging population, both by providing better preventative care and greater diagnostic capability [32], [33]. Wearable gait monitoring sensors and systems are also capable of providing quantitative and repeatable results over extended time periods [34]. As a result, gait analysis using wearable sensors has drawn researchers from many fields into searching for wearable means to effectively monitor human locomotion.

Existing wearables have demonstrated their value to health care through their use as a safe, cost-effective health care device in tracking physical activity [35]. North America accounts for almost 50% of wearable technology revenue and the market for wearable technology is projected to grow to over $70 billion by 2022 [36]. There are several popular existing health-monitoring wearables on the market including the Fit-bit, Apple Watch, and the Samsung Galaxy Active watch. A systematic review of these personal health care monitoring devices concluded that regardless of age, sex, and health status, people using wearables improved their amount of physical activity and daily steps [35]. Moreover, many of these wearables have been readily embraced for daily use, thus exemplifying customer demand for these technologies. Wearable devices can also be used to develop a personalized intervention based on the

user's goals and activity. Generally, users agree that wearable devices have positive value in promoting a healthy lifestyle [35] and the data collection function in these devices supports the development of customized interventions to promote wellness. In addition to promoting wellness, wearables have also provided early detection of anomalies and disease and facilitated early treatment and prevention of more serious health problems. A recent study found Fitbits and other wearables which monitor sleep and resting heart rate to be effective in detecting and tracking influenza out-breaks [37]. Ample anecdotal testimony attests to the ability of wearables to detect extremes in heart rate that prompt wearers to seek immediate medical treatment and avoid serious if not fatal health consequences of these episodes [38]. When used in conjunction with medical treatment, wearables can fast track adjustments and improvements in treatment. For example, wearable monitors have been successfully paired with medical treatment to monitor and optimize clinical interventions on patient mobility [39]. Despite problems with compliance and imperfect or incomplete data collection, wearables such as the Fitbit have also been successfully used to help depressed, alcohol-dependent women engage in lifestyle physical activity to resist their urge to drink during recovery [40]. Thus, it is no surprise that personal health care wearables and their potential to support improved and expanded access to health care have likely contributed substantially to the 14% increase in wearable device sales and the over 86 million wearable devices sold globally in the second quarter of 2020 [41].

On the other end of the spectrum, wearable gait monitoring systems used outside of a clinical setting are much less expensive and require far less power than their clinical counterparts. However, wearable systems are also inherently vulnerable to interference from a wide range of environmental and compliance factors. Further, the sensors on these devices often offer less accurate than those in clinical settings and the result is that the generated data have lower success rates in identifying abnormalities and irregularities in gait.

2.3. Gait Monitoring Technologies

Several wearable sensors for gait monitoring have been developed over the past two decades. A representative subset of these wearables is summarized in Table 2.1. A more thorough review of wearable sensors for gait monitoring can be found in [28], [30], [42].

Table 2.1. Wearable Sensors Used for Gait Analysis.

Year	Study	Sensors	Worn On	Function
2019	[43]	IMU	Ft	Measured stride width and stride length
2019	[44]	A	Ba	Measured toe-off and heel strike timing in the foot
2018	[45]	IR, IMU, F	Ft	Measured peak foot contact pressure, stance ratio, gait velocity
2017	[46]	F	Ft	Measured foot clearance for reducing falls among elderly
2017	[47]	IMG, EMG	L	Measured foot pressure distribution
2017	[48]	F	Ft	Evaluated gait asymmetry via foot contact pressure data
2015	[49]	IR	Ft	Measured foot position and orientation
2015	[50]	A	Ank	Measured multiple temporal gait parameters (e.g., cadence)
2015	[27]	F	Ft	Measured foot contact pressure during rehabilitation
2015	[51]	A, G, U	Ft	Measured step length and stride width
2014	[6]	IMU	S	Detected gait disturbances in Parkinson's disease patients
2014	[52]	IMU	H, Ba, L	Detected onset of a turn
2014	[53]	IMU	Ft, S, Th	Detected gait phases
2013	[54]	IMU, IR	Ft	Measured step length and stride width
2013	[55]	G	S	Measured stride length and gait velocity
2013	[56]	A	W	Detected Parkinsonian step and measure step length
2010	[57]	F	Ft	Detected abnormal gait using ground contact forces
2009	[58]	G, A	Ft, L	Detected gait phases
2008	[34]	A,B,EF, F, G	Ft	Detected gait abnormalities among Parkinson's disease patients
2007	[59]	F, IMU	Ft, L	Measured center of pressure, heel position, and ankle moment
2005	[60]	A, F	A, H, Ft, Sh, W	Detected gait abnormalities among diabetic patients
2004	[8]	G	Arm, Sh, Th	Detected gait abnormalities in Parkinson's disease patients
2003	[61]	F	Ft	Measured sheer and vertical forces in the foot during gait
2002	[62]	G	Sh, Th	Measured stride length and gait velocity
2002	[46]	F	Ft	Measured contact pressures and foot contact time for diabetics
2002	[63]	U	Ft	Measured stance/swing duration and step/stride length
1997	[64]	F,G	Th	Measured stride length and walking velocity

A (accelerometers); B (bend sensors); EF (electric field sensors); F (force/pressure sensors); G (gyroscopes); IR (infrared range sensors); U (ultrasonic range sensors); IMU (inertial measurement units); EMG (electromyography); Ank (ankle); Arm; Ft (foot); Ba (back); H (head); L (legs); Th (thigh); S (shank); Sh (shoulders); W (waist).

A vast majority of these wearables make use of a gyroscope (for measuring angular velocity and orientation), accelerometer, or inertial measurement unit (IMU—which combines a multi-axis gyroscope

and accelerometer and may also include a magnetometer) and are worn on the foot (shoe). For example, the GaitShoe uses an extensive suite of sensors including three accelerometers, three gyroscopes, four force sensors, and electric field sensors integrated into a sandal-like shoe that enables gait data to be collected unobtrusively over long periods of time and with minimal interference to normal gait [34]. Data regarding orientation, acceleration, and velocity collected from these accelerometers, gyroscopes, and IMU-based wearables on the foot have been successfully used to determine specific gait parameters including center of pressure in the foot [58], step length, and stride width [51]. Gyroscopes and accelerometers have been successfully employed to differentiate multiple different phases of human gait [41,46]. Wearables on the foot have also been used to fully capture and analyze foot motion [43], [54].

Accelerometers and gyroscopes are not the only sensors integrated into these wearable sensors. For example, researchers have developed a wearable gait tracking device for gait characteristics by implementing a set of force-sensitive resistors (FSR) to detect foot pressure at various locations on the underside of the foot and use that information to categorize six different stride positions during human gait known as heel strike, foot flat, heel off, terminal stance, and toe off [10]. Ultrasonic range sensors [51], [63], infrared sensors [42] , electric field [34], and electromyography (EMG) sensors for the detection of muscle activity during gait [47] have also been demonstrated in wearable gait sensors. These myriad sensors have been applied to the measurement of both temporal and spatial gait parameters achieving accuracies on the order of cm and sub-cm for spatial parameters (e.g., stride length, stride width, toe and heel position) and millisecond accuracy for temporal parameters (e.g., gait speed, cadence). Furthermore, several wearable sensors have also been demonstrated specifically for differentiating abnormal gait from normal gait (e.g., Table 2.2) with applications ranging from monitoring patients with Parkinson's disease [34] to recovery and rehabilitation from knee surgery [27].

Table 2.2. Wearable Sensors Used to Detect Abnormal Gait.

Study	Sensors	Worn	Approach
Arami et al [65]	HE	K	Linear and locally linear neuro-fuzzy estimators were used to translate the magnetic measures to accurately measure knee flexion-extension
Bamberg et al. [34]	A, B, EF, F, G	Ft	Pitch, stride length, stride time, and percent stance time used to differentiate normal and Parkinsonian gait
Djuric-Jovicic et al. [6]	IMU	S	Rule-based data processing used to detect normal, short, and very short strides as well as freezing of gait in Parkinson's disease patients
Laovoravit, et al. [66]	HE	Ft	Loading on the feet in normal and sheer directions were measured to treat diabetic foot ulcers
Li et al. [45]	IR, IMU, F	Ft	Peak pressure, stance ratio, stride length, walking velocity, and step-time variability used to compare toe-restrained vs. normal gait
Liu et al. [57]	F	Ft	Center of pressure and variation in foot contact forces used to detect fast, slow, and normal gait in obstacle and non-obstacle paths
Makino et al. [27]	F	Ft	Self-organizing maps (SOM) used to classify narrow vs. wide stride and slow vs. fast walking velocity for characterizing gait abnormality among patients who underwent total knee arthroplasty surgery
Petrofsky et al. [60]	A, F	Arm, H, Ft, Sh, W	Stance width and gait velocity found to be significantly different between normal and diabetic gait while walking a straight line and turning
Salarian et al. [8]	G	Arm, S, Th	Stride length and gait velocity; stance, double support, and gait cycle times used to detect abnormal gait among Parkinson's disease patients
Yu et al. [44]	A	Ba	Kurtosis, crest factor, and mean stride interval used to distinguish abnormal and normal gait in cerebralspinal mengingitis patients

A (accelerometers); B (bend sensors); EF (electric field sensors); F (force/pressure sensors); G (gyroscopes); HE (Hall-Effect Sensor); IR (infrared range sensors); IMU (inertial measurement units); Arm; Ft (foot); Ba (back); H (head); K (Knee); Th (thigh); S (shank); Sh (shoulders); W(waist).

Of particular interest to inexpensive and widely accessible gait monitoring wearables are Hall-effect sensors. These sensors are compact, inexpensive, have long lifetime, and with proper design, consume little power. They can be used to measure distances between objects (e.g., between the knees) and the presence or absence of objects (e.g., parts of the body) in a particular location. In previous research, Hall-effect sensors have been demonstrated in a few wearable systems. For example, four magnets embedded in silicon rubber were mounted in shoes above four Hall-effect sensors to measure the loading on the feet in normal and shear directions, which is often critical for properly treating diabetic foot ulcers [66]. Hall-effect sensors have also been used to estimate knee angle in prosthetics. A low-power magnetic measurement system based on two Hall-effect sensors and a magnet has been integrated into a smart knee prosthesis to accurately measure knee flexion-extension. Researchers used linear and locally linear neuro-

fuzzy estimators to translate the magnetic measures into knee flexion-extension while reducing power consumption for doing so by almost three-fold [65]. While limited, the demonstrated use of Hall-effect sensors for gait monitoring has been promising for monitoring a distinct subset of gait parameters which involve small distances on the order of cm or smaller. With this in mind, Hall-effect sensors were used to build a gait monitoring wearable. This literature search did not find any usage of Hall-effect sensors to measure gait parameters such as stride width and cadence.

2.4. This Study

Given the advantages of the Hall-effect approach, this study sought to explore the suitability of the Hall-effect sensor for capturing both cadence and leg gap (i.e., the distance between the legs at a particular location along the leg) as a proxy for stride width and stride width variability. The feasibility of using this system for detecting gait disturbances was evaluated using a prototype wearable sensor system that is mounted on the upper leg (i.e., thigh) just above the knee.

There are several benefits to the wearable Hall-effect magnet-based system developed in this effort. Upper leg wear is less vulnerable to abuse and premature wear and tear compared to sensors that are mounted on the bottom or side of shoes or the feet due to fewer mechanical stresses experienced along the upper leg. As one can imagine, sensors that are mounted on the inside of a shoe are subject to much higher mechanical abuse as the shoe is repeated lifted-up and stepped down, in contrast to that of a system mounted on the knee. This combined with the fact that Hall-effect sensors have no moving parts offers the possibility for a much longer lifetime in a corresponding wearable than classical alternatives that use accelerometers or gyros. Their high precision also allows for a more accurate detection of specific gait parameters. The system developed herein also demonstrated the use of a single sensor system to monitor gait in contrast to existing systems which typically rely on a combination of several different sensors and correspondingly use much more power and occupy more space at greater overall expense. For these reasons, Hall-effect sensors can provide gait monitoring that is accessible to a much broader population than existing systems, whether in an everyday or clinical setting.

Chapter 3

SYSTEM AND COMPONENT DESCRIPTION

As introduced in the previous chapter, there are significant benefits associated with the use of Hall-effect sensors in gait monitoring research and technology. This thesis will introduce a prototype of a wearable, gait sensing system for monitoring leg gap (stride width), leg gap (stride width) variability, cadence, and cadence variability using such technology. The prototype was designed, fabricated, and tested.

3.1 System Description

A block diagram of the sensor system designed to be worn at the knee and upper leg is shown in Figure 3.1. The system consists of four primary components: a *magnet*, *sensor* and sensor interface, *microcontroller* and supporting electronics, and *signal processing*. These four major components of the prototype system are described in detail in sections *3.1.1 Magnet* through *3.1.4 Signal Processing*.

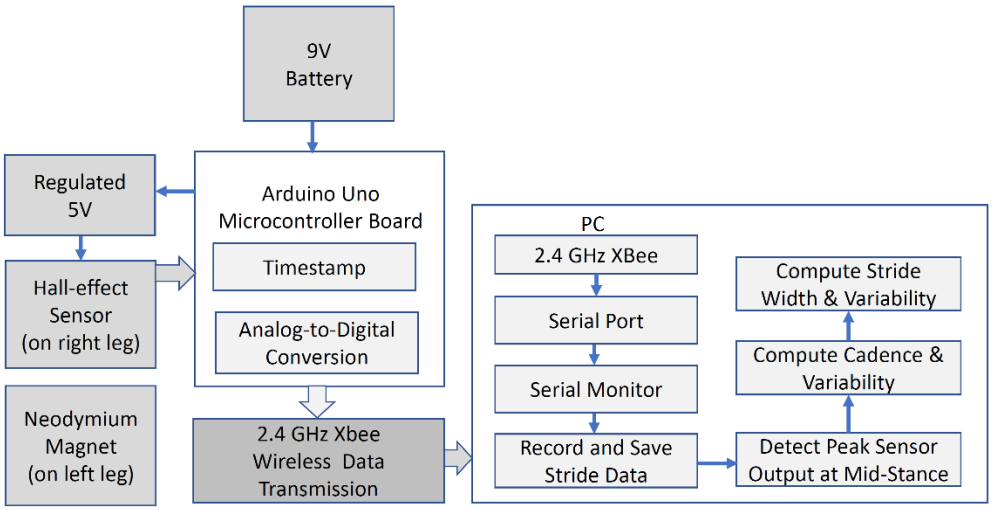

Figure 3.1. Block Diagram of Wearable Gait Monitoring System.

The critical components of this wearable system consist of a magnet and Hall-effect sensor. The Hall-effect sensor is powered by 5V supplied by the microcontroller and produces an analog voltage proportional to the distance between sensor and magnet. This signal is digitized by an Arduino Uno microcontroller and then wirelessly transmitted to a nearby computer (PC) using a 2.4 GHz Xbee for

signal processing to identify steps/strides, calculate leg gap and its variability (as a proxy for stride width), and compute cadence (steps per minute) and its variability.

For prototype testing purposes, the sensor, which was soldered onto a PCB board, was sewn on the outside of a lightweight knee brace (Figure 3.2) such that the face of the sensor was parallel to the leg and in close proximity to the opposite leg during mid-stance when the feet are together and on the ground. The magnet was mounted directly to the clothing using Velcro attached to elastic bandage on the opposite leg such that flat face of the ring magnet was parallel to the opposite leg and directly across from the Hall-effect sensor (Figure 3.2). This wearable prototype was used to evaluate whether this approach to gait monitoring could serve as a low-power, high-resolution means to capture a proxy for stride width and cadence. The footprint of the prototype system is quite large and would reduce by a factor of four or more in a fully integrated wearable system.

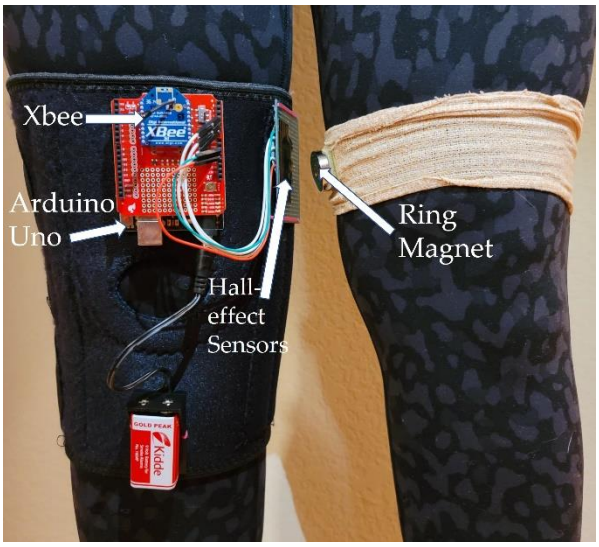

Figure 3.2 Prototype of Wearable Gait Monitoring System.

3.1.1 Magnet

A 2.54 cm diameter (0.794 cm inner diameter) N52 (Neodymium) ring magnet from KJ Magnetics was selected for integration into this wearable sensor system. Neodymium magnets are among the strongest magnets in the world and are made from neodymium, iron, and boron in $Nd_2Fe_{14}B$ structures [67]. The small ring magnet chosen for this sensor system produces a maximum magnetic field of 9400 Gauss (G)

at the outer edge of the ring magnet. In general, the magnetic field decreases with distance from the magnet. This relationship is described by the following equation for a ring magnet:

$$B_x = \frac{B_r}{2}\left(\left(\frac{x+T}{\sqrt{{R_o}^2+(x+T)^2}}-\frac{x}{\sqrt{{R_o}^2+x^2}}\right)-\left(\frac{x+T}{\sqrt{{R_i}^2+(x+T)^2}}-\frac{x}{\sqrt{{R_i}^2+x^2}}\right)\right) \quad (3.1)$$

where R_o is the outer radius of the magnet (2.54 cm); R_i is the inner radius of the magnet (0.794 cm); x is the distance from the sensor to the magnet surface, and T is the thickness of the magnet. B_x is the magnetic field at distance x from the surface of the magnet, and B_r is the surface magnetic field of the magnet as specified by the manufacturer in units of Gauss (G). This is illustrated in Figure 3.3 below.

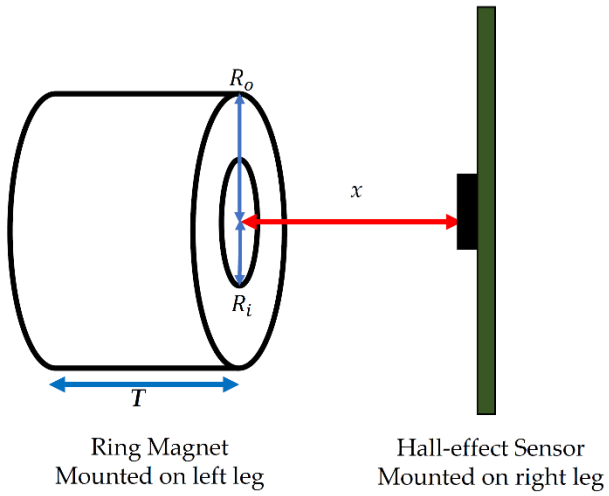

Figure 3.3. Sensor and Magnet Parameters.

Illustration of the magnet and its applicable parameters.

Fields as low as 3 G corresponding to distances that are approximately 0.27 cm away from the magnet are detectable with the Hall-effect sensor (Figure 3.4). Fields between 3-4 G corresponds to the detection limit imposed by the 10-bit analog-to-digital converter associated with the *microcontroller* in the wearable system that is responsible for converting the analog voltage produced by the Hall-effect sensor to its digital equivalent.

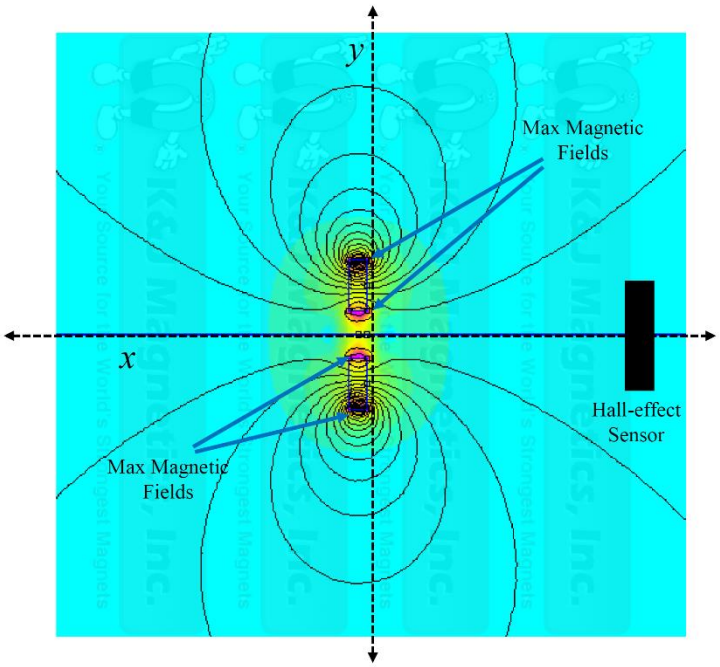

Figure 3.4. Magnetic Field (B) produced by N52 Ring Magnet [68]

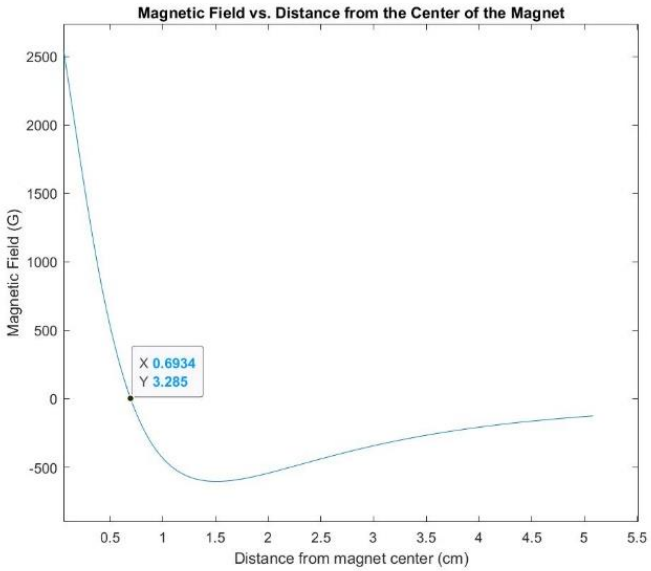

Figure 3.5. Magnetic Field (B) produced by N52 Ring Magnet [68]

Maximum magnetic field of 9400 Gauss are produced in each of the outer edges of the ring magnet while fields between 3-4 Gauss are produced up to 0.6 cm away from the flat surface of the ring magnet.

3.1.2 Sensor

A continuous-time ratiometric linear analog Hall-effect sensor manufactured by Allegro Microsystems (A1302) [69] was paired with the N52 ring magnet. The sensor generates an output voltage that is related to the detectable magnetic field as follows:

$$V_{out} = S \cdot B_x + V_{dd}/2 \tag{3.2}$$

where B_x is the magnetic field intensity at the sensor related to the distance between magnet and sensor as indicated in Equation 3.1, and S is the sensitivity of the magnet which ranges from 1.3 mV/G to 1.6 mV/G at a typical supply voltage of 5V. Equation 3.2 applies when the north pole of the magnet is located closest to the sensor. When the south pole of the magnet is in closer proximity, the output voltage is:

$$V_{out} = S \cdot -B_x + V_{dd}/2 \tag{3.3}$$

As seen from Equations 3.2 and 3.3, the output voltage linearly increases or decreases from the baseline voltage based on the polarity and the intensity of the ambient magnetic field.

The precision of the Hall-effect sensor used in this prototype system was determined experimentally through a calibration sequence. The north face of the magnet was placed parallel to the face of the sensor and the distance between the two was adjusted while maintaining the sensor location (distance b in Figure 3.6) along the x-axis (Figure 3.6) which passed through the middle of the hole in the center of the magnet. Because of the non-linear relationship between the magnet-sensor distance and the Hall output voltage, the sensor precision varied with distance. However, at a nominal distance of 1 cm corresponding to a leg gap of approximately 1.6 cm, the precision of the sensor system was +/- 0.07 mm which was determined by the inability of the 10-bit resolution of the analog to digital converter on the Arduino microcontroller to discern any smaller difference at this distance. The dynamic range of the sensor was estimated as 5 cm and was calculated as the distance between magnet and sensor at which a 0.16 cm increment in distance produced a change in the digital sensor output of less than two states (i.e., the resolution limit of the microcontroller).

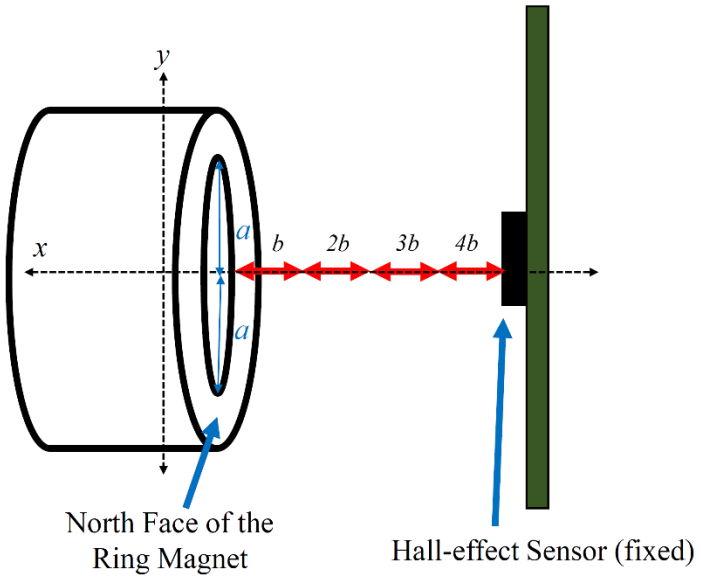

Figure 3.6. Diagram of precision measurement of the sensor

Precision of the magnet was determined experimentally through a calibration sequence. Distance 'a' is equal and illustrates that the sensor is at the center of the magnet on its x-axis. Distance b is used to calculate the precision of the magnet.

3.1.3 Microcontroller

An Arduino Uno microcontroller was used to collect analog voltage data from the Hall-effect sensor and digitize it. One 9 V battery provided power to the Arduino Uno microcontroller board which in turn provided a regulated 5 V output to the Hall-effect sensor. The Arduino Uno collected data from the sensor, timestamped the data, and transferred it to a 2.4 GHz Xbee for wireless transmission to a laptop computer (PC) for signal processing. Data were transferred at 57,500 baud. The Arduino Uno has a 10-bit on-board analog-to-digital converter which allows for $5/(2^{10}-1)$ or 4.9mV of resolution in reading the analog Hall-effect voltage. 4.9mV of resolution corresponds to a minimum detectable magnetic field of 4.9 Gauss for a sensor operating at minimum sensitivity (1.0mV/Gauss) and 3.1 Gauss for a sensor operating at maximum sensitivity (1.6mV/Gauss).

Raw data collected over the wireless Xbee connection were in the form of 10-bit digital signals representing sensor signals between 0 and 5 V. The ratiometric nature of the Hall-effect sensor forced the sensor output to $V_{dd}/2$ (i.e., 511 or 512 as a 10-bit digital signal) at zero magnetic field where V_{dd} is the

power supply (5 V) supplied to the sensor. The raw digital data were preprocessed to generate an analog voltage corresponding to the sensor output:

$$V_{out} = (5/1023) * \text{Digital Output} \quad (3.4)$$

3.1.4 Signal Processing

Data was recorded, saved, and analyzed in Matlab R2020A using the Statistics and Machine Learning toolbox. Signal processing of the data involved (a) preprocessing the data to identify peak outputs during gait that represented points in time when the legs were side-by-side (i.e., mid-stance peaks); (b) use of the timestamps corresponding to these points to compute cadence and cadence variability; and (c) extraction of these points to compute leg gap and variability using three different methods (Theory-based Methods 1 and 2 and Empirical Method 3). In this thesis, leg gap was calculated using three different methods. These three different methods were used to compute leg gap (i.e. a proxy for stride width) from the digital output generated by the Arduino Uno microcontroller. Theory-based methods 1 and 2 were based on underlying Hall-effect sensor and magnetism theory and used the manufacturer-specified maximum sensitivity of the Hall-effect sensor of 1.6 mV/Gauss and the minimum sensitivity of the Hall-effect sensor of 1.3 mV/Gauss. Empirical method 3 used experimental calibration data. Further detail of these methods is provided in *Section 4.3.1 Calculation of Leg Gap (Stride Width) using Methods 1 and 2* and *Section 4.3.2 Calculation of Leg Gap (Stride Width) using Method 3*. Further explanation of items (a) through (b) will be identified *in Section 4.1 Data Condition and Preprocessing*.

3.2 Experimental Design

The goal of testing and data collection at this phase in the research was proof of concept, leading to two research questions:

RQ1: Can the wearable system capture cadence with sufficient accuracy to differentiate abnormal and irregular strides from normal strides?

RQ2: Does leg gap captured using the wearable system make a sufficient proxy for stride width in terms of differentiating abnormal and irregular strides from normal strides?

To evaluate these two research questions, the gait monitoring system prototype was tested on four individuals walking with five different types of gaits.

For the purpose of experimental study, five different types of gaits were selected and defined. A baseline gait, defined as *normal* gait, was defined as the individual's normal pace and stride type; the gait should be automatic, and without conscious attention or focus on the speed or nature of the gait. In contrast to normal gait, two additional stride categories were constructed: *abnormal and irregular* strides. *Abnormal* strides were simulated by asking each individual to walk at a brisk or fast stride compared to their normal pace and then at a pace that was slow compared to what each individual considered normal or natural. These abnormal gait types were then defined as *fast* and *slow* strides, respectively. Limping strides (on both left and right sides of the body) were used to represent *irregular* strides and were simulated by asking each individual to walk with the left shoe off (right antalgic) or with the right shoe off (left antalgic). Antalgic gait is a form of irregular gait which is typically developed to avoid pain by walking (i.e., a limp). It is defined as a gait where the stance (i.e., foot on the ground) phase of the affected leg is shortened relative to the swing phase as compared to normal or healthy gait. To reduce or avoid pain, the subject spends most of their stance time with their weight being placed on the normal or healthy leg. In antalgic gait, the swing phase is increased on the affected side and may be shortened on the normal leg in order to get the normal leg back to the ground [33]. In this way, irregular strides were represented by right antalgic and left antalgic gaits. Table 3.1 summarizes the five gait types selected and constructed to test the gait monitoring prototype.

Table 3.1. Gait Types Used to Test the Prototype Gait Monitoring System.

Gait Label	Type	Description
Normal	Normal	Walk at a normal pace, one that requires no conscious attention or focus on the nature or speed of gait.
Fast	Abnormal	Walk at a brisk pace, as if in a hurry.
Slow	Abnormal	Walk slowly, as if enjoying a sunny day.
Right antalgic	Irregular	Walk in such a way that stance/swing ratio on the right side of the body is smaller than normal gait—by walking with the left shoe off. Simulates a right limp.
Left antalgic	Irregular	Walk in such a way that stance/swing ratio on the left side of the body is smaller than normal gait—by walking with the right shoe off. Simulates a left limp.

3.2.1. Testing Procedures

The Hall-effect prototype was tested on four individuals walking with the five different types of gait. The different types of gaits were intended to test abnormal and irregular gaits, for example, abnormal (fast and slow) and irregular gaits (right antalgic and left antalgic) strides. For each subject test, the individual walked six different segments consisting of approximately 10 m each on smooth concrete in the second-floor atrium in the Electrical Engineering building at the University of Washington Seattle, for a total of 60 m walked for each of the five types of gait per individual (Table 3.1).

For the purposes of this research, note that subjects' gait was not compared between subjects, but only within subjects because that what is considered a "normal" stride is unique to a particular individual. For example, the normal cadence of an Olympic athlete is likely very different than the average person due to differences in fitness level and athletic ability. Therefore, what is "normal" for an Olympic athlete may very well be "abnormal" for another person. Since the intent of this research was to be able to identify when and how a subject's gait transitioned from normal to abnormal, there was no need to compare data between subjects.

The four individuals from whom data were collected were all students or instructors in an independent study course focused on gait monitoring. As a result, the authors' home institution determined that this study was not human subjects research and did not require institutional review board (IRB) approval.

Complete data were collected in a single session in December of 2019 and were analyzed as described in Chapter 4, next.

Chapter 4
SIGNAL PROCESSING

In this section, this thesis will explore the methods and necessary theory to calculate the two previously identified gait parameters: stride width and cadence. Variability in stride width has been found to be a reliable indicator for a variety of ailments. Research has shown that stride width variability is especially important for diagnosis and monitoring of injury, potential injury, and disease including neurological disease, cognitive impairment, balance control and gait stability, and increased fall risk. Similarly, research has shown that gait disturbances in cadence can be linked to a variety of injuries and disease such as visual impairment, depression, risk of injury among runners, and the prevention of injury. In addition, cadence also serves as an important context for studying other gait parameters. In many gait monitoring studies, cadence is used as a baseline parameter for the study of other gait parameters, including that of stride width.

4.1 Data Condition and Preprocessing

For calculation of both leg gap (stride width) and cadence, the data communicated by the Xbee from the wearable Hall-effect sensor system is first back calculated from digital output to an analog voltage. Among the five groups of strides and four subjects evaluated, the number of strides recorded for each segment varied with the type of gait, individual, speed of gait (cadence), and stride length. Once the raw digital data has been preprocessed to generate an equivalent analog voltage, the data is then conditioned for the identification of midstance peaks.

4.1.1. Identification of Mid-Stance Peaks

Data was preprocessed and filtered to identify mid-stance peaks. The mid-stance peak corresponds to the point at which the legs are closest together and both feet are on the ground in the middle of astride. When the legs are closest together, the Hall-effect sensor produces a maximum or minimum output depending on the polarity of the magnet relative to the Hall-effect sensor. To eliminate the impact of variations in swing between the two legs, leg gap was calculated at the mid-stance peak associated with each step

involving only the swing of the left leg. Depending on the orientation of the magnet, these mid-stance peaks could be identified as either local maxima or minima. However, in order to reduce confusion during the following explanation, these peaks will be consistently referred to as "maxima."

In order to reduce the occurrence of false, local maxima in the raw data, mid-stance peaks were identified in the sensor output as local maxima that were at least 0.8 seconds apart. This minimum separation corresponds to a maximum detectable cadence of 150 steps/min, well above the 115-120 steps/min at which a typical adult walks. Once these local maxima were identified, the sensor output was filtered by replacing all data that did not correspond to one of these local maxima with the value of the sensor baseline, essentially zeroing the non-maxima values out. Then, the local maxima were filtered by their prominence in order to eliminate spurious, low-signal maxima that did not represent mid-stance peaks. While this approach eliminated some valid mid-stance peaks, it ensured that very few false peaks remained in the data. Thus, the remaining identified maxima were identified as true mid-stance peaks. In the representative raw (analog voltage) data shown in Figure 4.1, true mid-stance peaks are marked with a black asterisk and anomalies and false local maxima are marked with red asterisks. These false local maxima (red asterisks) were often found to be noise generated from turns during subject testing.

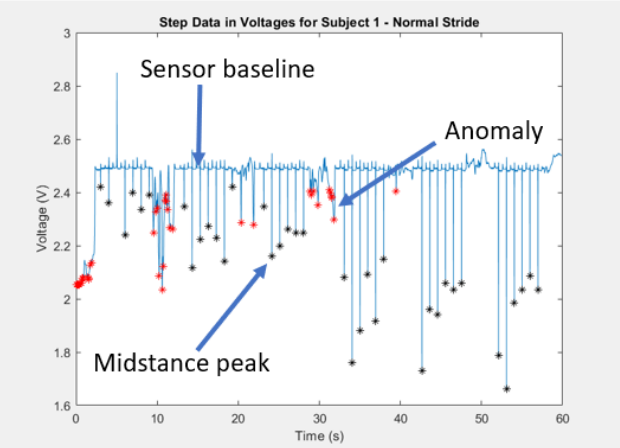

Figure 4.1. Example of Step data and Identified Midstance Minima

This figure identified the local minima in subject 1. Subject one was the only subject which had the south face of the magnet facing towards the sensor, which resulted in minima. The sensor baseline is illustrated as well as an example of the anomalies (red asterisk) in the data. These were not considered midstance peaks (black asterisk) due to their low signal or did not meet cadence criteria.

Once identified by time (of occurrence) and analog voltage, these mid-stance peaks are used in the calculation of both cadence and leg gap (as a proxy for stride width).

4.2 Calculation of Cadence

Mid-stance peak correlations occur within specific gait phase (see Figure 4.2). Gait phases are often used to model gait cycles. These gait phases can vary but are typically accepted as: heel-strike, foot-flat, mid-stance, push-off, acceleration, mid-swing and deceleration. As illustrated from Figure 4.2, mid-stance in the data is detected as a large, high magnitude peak in the voltage data. Mid-swing, another gait cycle at which the legs are side-by-side occurs with a lower peak that is opposite in direction (e.g. negative) to the mid-stance peak.

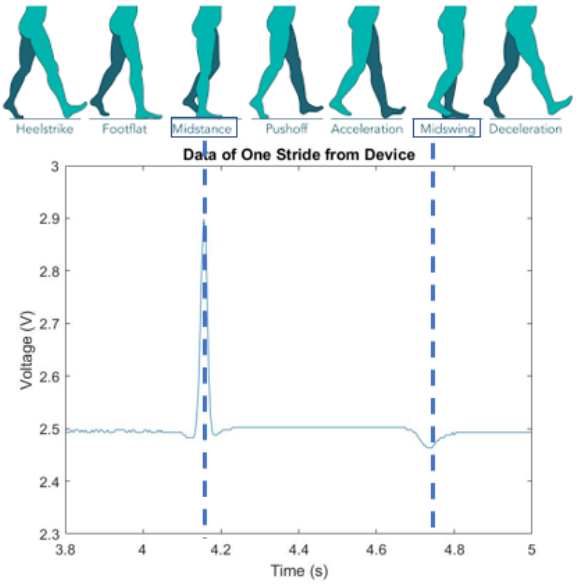

Cite https://www.tekscan.com/blog/medical/gait-cycle-phases-parameters-evaluate-technology

Figure 4.2. Mid-stance and Mid-swing stances and Voltage Data

This figure illustrates the gait phases in relation to a step as measured by the system.

Once mid-stance peaks were identified in the data, their timestamps were used to calculate cadence. Strides per minute were calculated simply as the reciprocal of adjacent mid-stance peaks (in sec) and

scaled to minutes: where t_n is the time at which a mid-stance peak occurs for stride n and t_{n-1} is the time at which a mid-stance peak occurs for the stride immediately before stride n. Although a stride is formally defined as the time between two consecutive heel strikes on the same foot (Figure 4.3), the time between two mid-stance peaks was estimated as equivalent to one stride.

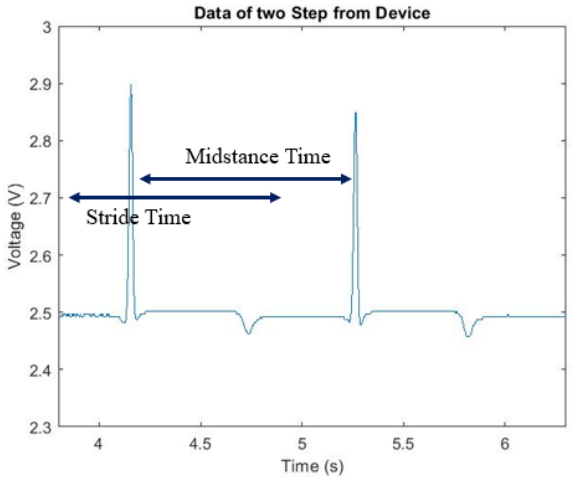

Figure 4.3. Mid-stance time vs. Stride Time to Calculate cadence.

By convention, stride time is defined as the time between two consecutive heel strikes of the same foot. Stride time is estimated in the figure above because this system was not able to identify the heel strike gait phase from the data. In this work, mid-stance time was calculated as an accurate estimate of stride time.

Strides per minute were then calculated as:

$$Strides\ per\ minute = 60/(t_n - t_{n-1}) \tag{4.1}$$

Since one stride is equal to two steps, cadence in steps per minute could be easily estimated as:

$$Cadence = 2 \cdot Strides\ per\ minute \tag{4.2}$$

Variability in cadence was then calculated as the standard deviation of all cadences calculated for a particular individual (subject) and type of gait. The mid-stance peaks were also used to calculate leg gap (the distance between the two legs at the point where the sensor and magnet were mounted), described next.

4.3 Calculation of Leg Gap (Stride Width)

Stride width variability is identified in the literature as an important means to detect gait disturbances, however this study explores the use of leg gap as a proxy for stride width. While stride width is measured as the distance between two imaginary parallel lines passing through the heel of the foot, leg gap is measured as the distance between the legs slightly above the knees where the Hall-effect sensor and magnet were worn during testing. It is assumed that leg gap makes a sufficient proxy for stride width, as leg gap and stride width is consistent per subject. In this section, the calculation of leg gap will be explained as a proxy for stride width. Three distinct methods were evaluated for calculating leg gap, described next.

4.3.1 Calculation of Leg Gap (Stride Width) using Methods 1 and 2

Methods 1 and 2 calculated leg gaps based on theoretical behavior of the sensor and of the magnet. The digital output of the sensor system was first processed to generate an analog voltage that represented the Hall-effect sensor output. Once converted to voltage, magnetic field B_x was calculated from the theoretical behavior of the Hall-effect sensor as follows:

$$V_{out} = S \cdot B_x + V_{dd}/2 \tag{4.3}$$

Methods 1 and 2 are different only in the sensitivity S used to calculate B_x. Method 1 uses the maximum sensitivity or 1.6 mV/G as specified in the manufacturer datasheet and Method 2 uses the minimum sensitivity of 1.3 mV/G. The supply voltage V_{dd} is a regulated and stable 5V.

Once the magnetic field B_x is known, the distance x between magnet and sensor (which is critical to calculating the leg gap) can be calculated. To do this, it is assumed that the maximum sensor output occurs when the Hall-effect sensor is located along the line/axis passing through the center of the magnet (see Figure 3.4). The distance x can then be calculated using the known properties of the magnet:

$$B_x = \frac{B_r}{2}\left(\left(\frac{x+T}{\sqrt{{R_o}^2+(x+T)^2}} - \frac{x}{\sqrt{{R_o}^2+x^2}}\right) - \left(\frac{x+T}{\sqrt{{R_i}^2+(x+T)^2}} - \frac{x}{\sqrt{{R_i}^2+x^2}}\right)\right) \quad (4.4)$$

Unfortunately, x cannot be calculated directly from Equation 4.4 and is instead calculated iteratively based on a value of magnetic field B_x estimated from Equation 4.3. The conversion of digital output to leg gap is illustrated graphically in Figure 4.4.

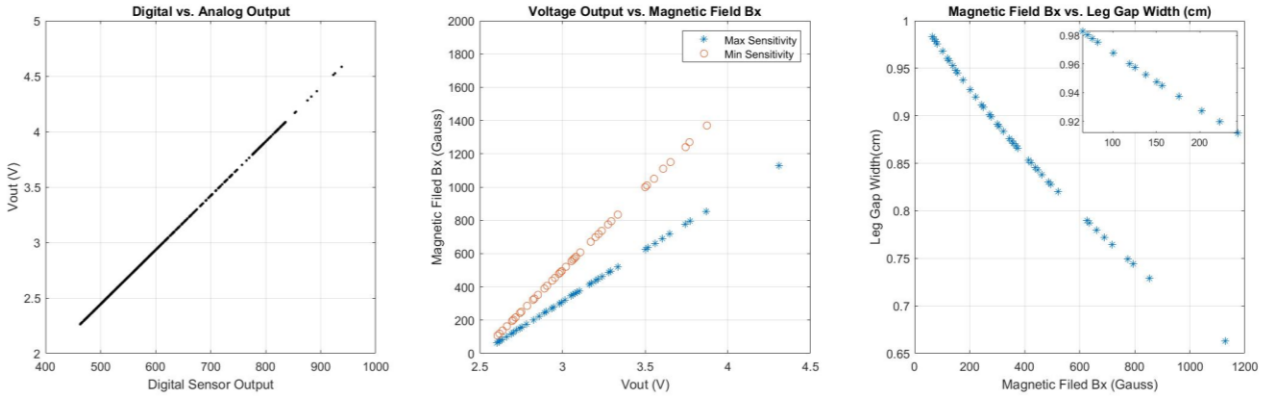

Figure 4.4. Relationships between Sensor System Output and Leg Gap.

Graphs of digital to analog input (1), and voltage output to magnetic field (3) and magnetic field to leg gap (left to right) (3). Graph (3) has an inlet of leg gaps of less than 250 gauss. Note: Data shown is experimental. Voltage measurement was taking using the north-facing magnet, which resulted in maxima, and thus illustrates voltages of 2.5V and up.

Once the distance x is known, the leg gap (i.e., the distance between the legs at the point where the sensors are mounted) can then be estimated as:

$$Leg\ gap = x + T + W_{Sensor+Board} \quad (4.3)$$

where $W_{Sensor+Board}$ is the sum of the width of the sensor and the width of the printed circuit board on which the sensor is mounted and T is the thickness of the magnet (as shown in Figure 3.4).

4.3.2 Calculation of Leg Gap (Stride Width) using Method 3

In the third method, leg gap is calculated using experimental data collected as shown in Figure 4.5 below.

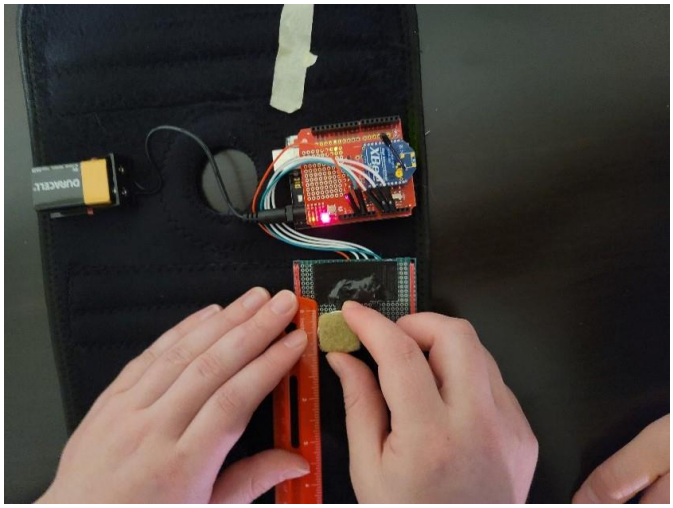

Figure 4.5. Empirical Calibration of Lap Gap values.

After preprocessing data initially from digital output to analog, this voltage data was then compared to empirically calibrated data. Calibration was calculated by observing voltage output at set distances from the sensor. The magnet was placed at ascending distances away from the Hall-effect sensor, and digital sensor output was then recorded at these set distances. Data measurements and their interpolated values from empirical calculation of leg gap using method 3 is shown in Figure 4.6.

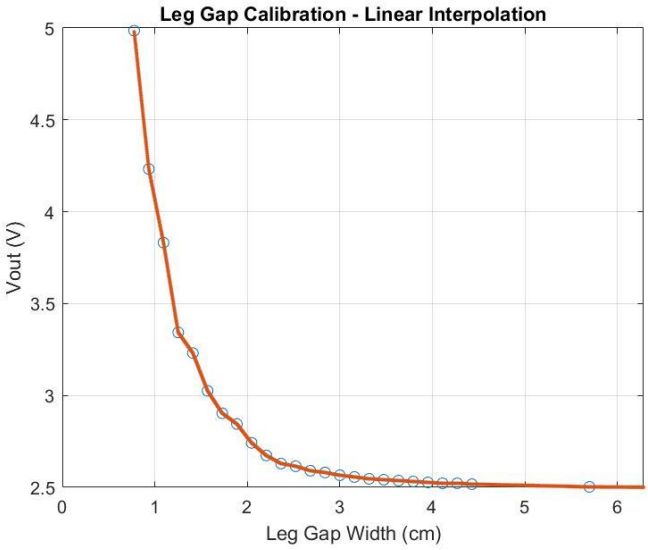

Figure 4.6. Linear interpolation of Calibrated Lap Gap values.

Leg gap is calculated by interpolating calibration values and adding the width of the sensor and board, and the thickness of the magnet. Interpolated values are indicated by the solid line in the graph.

Calibration data were then used to create a look-up table containing leg gap data vs analog sensor outputs (V_{out}) in Equation (3.1) in 0.001 m increments. Linear interpolation was used to generate leg gap between adjacent calibration points. Stride can then be calculated from subject data by comparing the nearest calibrated output voltage. This method replaces runtime computation with a supplier array indexing operation, which in turn reduces processing time.

A summary of the three different methods of leg gap (stride width) calculation can be summarized in table 4.1 below and data comparing the differences in leg gap distance between methods 1, 2, and 3 are illustrated in Table 5.5 and Table 5.6 in Chapter 5.

Table 4.1. Summary of Methods of Leg Gap Calculation.

Method #	**Type of Leg Gap Calculation**
1	Theoretically calculated using max sensitivity
2	Theoretically calculated using min sensitivity
3	Empirically Calculated using Experimental Data

4.4. Statistical Tests: Introduction to the Kruskal-Wallis test by ranks and Levene Test for Equality of Variances

Once calculated, cadence, and leg gap (as a proxy for stride width) were used to evaluate differences among stride types among all four individuals tested. The intent of the above data analysis was to understand whether the data collected by the wearable sensor system was capable of distinguishing abnormal gait (fast, slow) and irregular gait (right antalgic, left antalgic) from normal gait via differences in cadence, differences in leg gap, differences in leg gap variability, differences in cadence variability, or some combination thereof. Thus, appropriate statistical tests were then used to assess whether the null hypothesis that an abnormal or irregular gait for a given subject was the same as a normal gait could be rejected.

The following two statistical tests were selected due to their compatibility with the data. Normality was tested using a Lilliefors test which is based on the Kolmogorov–Smirnov test for normality. The Lilliefors test assessed whether the null hypothesis that the sample data came from a normal parent population could be rejected at the 0.05 confidence level [65]. Because a significant amount of the data (43% of maximum and minimum sensitivity leg gap groups) was shown to not be non-parametric or not normal, the Kruskal-Wallis test by ranks and Levene Test for Equality of Variances were identified for use in this thesis.

4.4.1 The Kruskal-Wallis test by Ranks

Kruskal–Wallis test by ranks H test, also known as one-way ANOVA on ranks, is a method for testing whether samples originate from the same distribution. It is used for comparing two or more independent samples of equal or different sample sizes. The Kruskal–Wallis test by ranks is a non-parametric test that compares the medians rather than the means of different sample populations and does not rely on assumptions of normality for accuracy [70]. This same test was used to evaluate whether cadence associated with each abnormal or irregular stride was significantly different from that associated with normal. Additionally, it was also used to evaluate whether leg gaps for abnormal or irregular stride was significantly different than the leg gaps associated with normal stride for the same individual.

4.4.2 The Levene Test for Equality of Variances

The second statistical method for evaluation of experimental data was Levene Test for Equality of Variances. Levene Test for Equality of Variances p-test assesses the equality of variances for a variable calculated for two or more groups. Levene Test for Equality of Variances evaluates that the null hypothesis that the population variances of the populations from which the different samples are drawn are equal [71]. Like that of the Kruskal-Wallis test by ranks, Levene Test for Equality of Variances uses data that comes from a non-normal distribution. This test was used to assess if the variability of cadence could be used to identify abnormal or irregular gaits. Moreover, the variability in leg gap was evaluated using a Levene Test for Equality of Variances which compared the variances of leg gaps and determined

whether the null hypothesis that strides varied similarly for an abnormal or irregular stride as for a normal stride could be rejected.

Chapter 5

RESULTS

The Hall-effect sensor-based gait monitoring system was used to detect abnormalities and irregularities in walking by sensing leg gap and cadence along with their variabilities. The system was implemented slightly above the knees and leg gap was used as a proxy for stride width. As illustrated in the previous chapters, the wearable system was tested on four different individuals and five different types of gait: normal, abnormal (fast, slow), and irregular (right antalgic, left antalgic). In this chapter, the test results will be presented, and the previously raised research questions will be answered in Chapter 6.

Normality was evaluated using the Lilliefors Test which evaluates the null hypothesis that data comes from a normally distributed population. The Lilliefors test is based on the Kolmogorov–Smirnov test which is used to test if the sample is drawn from the reference by quantifying a distance from the empirical distribution of the sample and the cumulative distribution function of the reference function [72]. For the purposes of this thesis, the Lilliefors test was used to determine the appropriate statistical tests to use, specifically on whether to assume normally distributed data or not (Table 5.1 and Table 5.4).

5.1 Statistical Results of Cadence Parameters

Descriptive statistics for the cadence associated with five types of strides for each of four subjects are summarized in Table 5.1. Variability in cadence was measured using four variability parameters: maximum (max), minimum (min), interquartile range (IQR), and standard deviation (SD). Skewness and kurtosis were also calculated, as well as normality.

Table 5.1. Descriptive Statistics and Normality of Cadence Data.

Type	N*	Cadence [Steps/Min]					Skewness	Kurtosis	Normal **
		Mean	SD	IQR	Max	Min			
Subject #1									
Normal	29	122.22	2.06	3.13	125.92	117.42	−0.37	2.73	Y
Fast	27	127.97	3.45	2.35	133.33	116.39	−2.07	7.73	N
Slow	33	100.74	2.54	3.15	105.45	95.16	−0.49	2.78	Y
AntalgicR	30	121.15	2.32	2.68	125.66	116.73	0.25	2.47	Y
AntalgicL	34	120.50	3.03	4.47	125.13	113.74	−0.59	2.39	N
Subject #2									
Normal	41	117.15	3.64	4.12	127.52	108.11	0.39	4.36	Y
Fast	32	134.17	4.34	3.77	145.81	129.31	1.49	4.72	N
Slow	43	110.33	2.97	3.63	121.09	104.26	0.50	5.61	N
AntalgicR	36	118.75	4.06	4.86	124.74	108.50	−0.82	3.29	Y
AntalgicL	42	119.34	2.85	2.96	126.58	112.36	0.29	3.54	Y
Subject #3									
Normal	43	110.75	3.73	4.55	117.76	101.35	−0.67	3.24	N
Fast	35	119.41	4.39	4.78	132.01	111.32	0.66	3.79	Y
Slow	48	77.44	3.30	3.57	86.15	70.01	−0.24	3.33	Y
AntalgicR	44	108.44	4.14	4.59	120.48	99.50	0.48	4.52	Y
AntalgicL	43	107.77	4.01	4.01	115.72	99.09	−0.14	2.36	Y
Subject #4									
Normal	32	118.40	2.93	4.40	123.33	111.63	−0.63	2.98	Y
Fast	26	141.06	4.72	7.40	149.25	130.72	−0.24	2.43	Y
Slow	28	105.53	4.95	7.07	115.16	97.56	0.10	2.27	Y
AntalgicR	29	125.10	4.00	6.14	132.01	115.72	−0.43	2.78	Y
AntalgicL	35	125.26	2.53	2.98	129.31	119.28	−0.46	2.88	Y

*N is the number of peaks.

**Evaluated using the Lilliefors (based on Kolmogorov–Smirnov test) normality test.

Five of 20 sample distributions failed the Lilliefors normality test. Therefore, the subsequent statistical tests for cadence and cadence variability did not assume a normal distribution. Out of 20 groups of data

(i.e., five groups for each of four subjects), only 2 (10%) were highly skewed with an absolute value greater than 1. Five (25%) were moderately skewed with absolute values between 0.5 and 1, and the remaining 13 (65%) distributions were approximately symmetric with skewness values ranging between −0.5 and 0.5. Most data groups (12 of 20) were negatively skewed. Only five of the distributions have kurtosis >4 which means these five distributions were much more peaked than a normal distribution.

Results of the non-parametric Kruskal–Wallis test by ranks used to compare the cadence of abnormal (fast, slow) or irregular (right antalgic, left antalgic) strides to normal strides are summarized in Table 5.2. In all (100%) of comparisons, the tests detected that strides that were not normal were significantly different than normal strides.

Table 5.2. Detection of Abnormal or Irregular Strides using Cadence [steps/minute] (Kruskal–Wallis test by ranks).

Subject	Fast Strides		Slow Strides		Right Antalgic		Left Antalgic	
1	H (1) = 30.10 p = 0.000	***	H (1) = 45.60 p = 0.000	***	H (1) = 3.89 p = 0.049	*	H (1) = 5.03 p = 0.025	*
2	H (1) = 53.20 p = 0.000	***	H (1) = 47.95 p = 0.000	***	H (1) = 5.16 p = 0.023	*	H (1) = 10.11 p = 0.000	***
3	H (1) = 46.62 p = 0.000	***	H (1) = 67.32 p = 0.000	***	H (1) = 10.86 p = 0.001	**	H (1) = 11.09 p = 0.0009	***
4	H (1) = 42.32 p = 0.000	***	H (1) = 41.57 p = 0.000	***	H (1) = 31.17 p = 0.000	***	H (1) = 43.36 p = 0.000	***

Cadence of Stride is significantly different from normal (* $p < 0.05$; ** $p < 0.01$; *** $p < 0.001$).

The Levene test for Equality of Variances was also used to compare cadence variability between types of strides. Variability in cadence was not particularly useful in differentiating strides (Table 5.3). The Levene Test for Equality of Variances rejected the null hypothesis that the variance of a stride that was not normal was equal to that of normal stride in only three of 16 cases (19%).

Table 5.3. Detection of Abnormal or Irregular Strides Using Cadence Variability (Levene Test for Equality of Variances).

Subject	Fast Strides	Slow Strides	Right Antalgic	Left Antalgic
1	$F = 0.53$ $p = 0.487$	$F = 0.90$ $p = 0.347$	$F = 0.47$ $p = 0.496$	$F = 5.48$ $p = 0.023$
2	$F = 0.36$ $p = 0.551$	$F = 0.48$ $p = 0.402$	$F = 1.04$ $p = 0.312$	$F = 0.92$ $p = 0.341$
3	$F = 0.41$ $p = 0.524$	$F = 9.35$ $p = 0.493$	$F = 0.09$ $p = 0.763$	$F = 0.89$ $p = 0.345$
4	$F = 7.57$ ** $p = 0.008$	$F = 6.69$ ** $p = 0.0013$	$F = 3.33$ $p = 0.073$	$F = 0.65$ $p = 0.424$

* $p < 0.05$; ** $p < 0.01$; *** $p < 0.001$.

5.2 Statistical Results of Leg Gap Parameters

A second gait parameter, leg gap, was also evaluated using similar statistical tests that were used to evaluate cadence (steps per minute). Three different methods were used to compute leg gap from the digital output generated by the Arduino Uno microcontroller (Table 5.4 – 5.8). Methods 1 and 2 were based on underlying Hall-effect sensor and magnetism theory and used the manufacturer-specified maximum sensitivity of the Hall-effect sensor of 1.6 mV/Gauss and the minimum sensitivity of the Hall-effect sensor of 1.3 mV/Gauss, respectively. Method 3 used experimental calibration data collected as described in Chapter 4, Section *4.3.2 Calculation of Leg Gap (Stride Width) using Method 3*.

Descriptive statistics for the leg gap calculated using theory (Methods 1 and 2) are summarized in Table 5.4 and 5.5. Table 5.4 illustrates distribution characteristics for both Methods 1 and 2; normality of data distributions were evaluated using the Lilliefors normality test. Table 5.5 provides descriptive statistics for Methods 1 and 2.

Table 5.4. Normality Data for Leg Gap calculated using Methods 1 (for maximum sensitivity) and 2 (for minimum sensitivity)

		Parameters associated with maximum (minimum) sensor sensitivity			
Subject	Stride	N*	Skewness	Kurtosis	Normal**
#1	Normal	37	−0.24 (-0.223)	2.33 (2.271)	Y (Y)
	Fast	38	0.22 (0.268)	2.54 (2.576)	Y (Y)
	Slow	48	-1.60 (-1.541)	5.61 (5.477)	N (Y)
	Right Antalgic	37	-1.09 (-1.104)	3.43 (3.478)	N (N)
	Left Antalgic	40	-0.67 (-0.624)	2.55 (2.508)	N (N)
#2	Normal	44	-2.50 (-2.365)	13.5 (12.65)	N (N)
	Fast	38	-1.12 (-1.078)	3.91 (3.732)	N (N)
	Slow	44	-0.43 (-0.356)	4.4 (3.266)	Y (N)
	Right Antalgic	42	−1.01 (-0.908)	5.64 (5.42)	Y (Y)
	Left Antalgic	46	−1.60 (-1.49)	5.86 (5.504)	N (N)
#3	Normal	51	−0.68 (-0.543)	3.08 (2.861)	Y (Y)
	Fast	41	−0.25 (-0.152)	2.91 (2.918)	Y (Y)
	Slow	53	−0.83 (-0.717)	3.68 (3.41)	Y (Y)
	Right Antalgic	50	−0.84 (-0.776)	5.13 (5.065)	Y (Y)
	Left Antalgic	49	−0.55 (-0.467)	3.18 (3.043)	Y (Y)
#4	Normal	38	−0.46 (-0.343)	3.26 (3.046)	Y (Y)
	Fast	32	−1.01 (-1.143)	3.45 (3.73)	N (N)
	Slow	34	−0.81 (-0.836)	3.33 (3.296)	Y (Y)
	Right Antalgic	36	−0.89 (-0.869)	3.07 (3.099)	N (Y)
	Left Antalgic	41	−3.11 (-3.007)	17.1 (16.231)	N (N)

*N is the number of peaks.
* Evaluated using the Lilliefors (based on Kolmogorov–Smirnov test) normality test.

Table 5.5. Descriptive Statistics for Leg Gap calculated using Methods 1 and 2

		Parameters associated with maximum (minimum) sensor sensitivity					
Subject	Stride	N*	Mean	SD	IQR	Max	Min
#1	Normal	37	1.53 (1.486)	0.046 (0.065)	0.057 (0.081)	1.61 (1.59)	1.44 (1.349)
	Fast	38	1.42 (1.332)	0.09 (0.124)	0.114 (0.155)	1.59 (1.57)	1.24 (1.085)
	Slow	48	1.5 (1.441)	0.091 (0.127)	0.099 (0.14)	1.61 (1.598)	1.12 (1.021)
	Right Antalgic	37	1.41 (1.313)	0.089 (0.124)	0.086 (0.114)	1.52 (1.466)	1.46 (1.021)
	Left Antalgic	40	1.55 (1.507)	0.04 (0.057)	0.061 (0.088)	1.29 (1.598)	1.14 (1.374)
#2	Normal	44	1.58 (1.557)	0.017 (0.026)	0.017 (0.023)	1.61 (1.6)	1.5 (1.435)
	Fast	38	1.59 (1.561)	0.023 (0.033)	0.025 (0.041)	1.61 (1.6)	1.52 (1.466)
	Slow	44	1.58 (1.553)	0.016 (0.024)	0.025 (0.039)	1.61 (1.595)	1.53 (1.481)
	Right Antalgic	42	1.48 (1.413)	0.065 (0.033)	0.079 (0.112)	1.6 (1.588)	1.25 (1.092)
	Left Antalgic	46	1.55 (1.504)	0.048 (0.067)	0.036 (0.053)	1.61 (1.6)	1.37 (1.265)
#3	Normal	51	1.49 (1.425)	0.074 (0.103)	0.088 (0.13)	1.6 (1.583)	1.28 (1.136)
	Fast	41	1.47 (1.391)	0.072 (0.1)	0.093 {0.128)	1.62 (1.608)	1.29 (1.151)
	Slow	53	1.53 (1.482)	0.054 (0.076)	0.071 (0.102)	1.62 (1.608)	1.36 (1.247)
	Right Antalgic	50	1.48 (1.403)	0.063 (0.1)	0.071 (0.099)	1.6 (1.578)	1.25 (1.087)
	Left Antalgic	49	1.51 (1.455)	0.05 (0.071)	0.064 (0.088)	1.61 (1.598)	1.38 (1.275)
#4	Normal	38	1.53 (1.482)	0.044 (0.062)	0.064 (0.094)	1.61 (1.593)	1.41 (1.308)
	Fast	32	1.6 (1.587)	0.012 (0.018)	0.013 (0.018)	1.62 (1.613)	1.57 (1.54)
	Slow	34	1.59 (1.569)	0.016 (0.024)	0.018 (0.028)	1.61 (1.603)	1.55 (1.507)
	Right Antalgic	36	1.61 (1.595)	0.011 (0.018)	0.017 0.024)	1.62 (1.613)	1.58 (1.552)
	Left Antalgic	41	1.62 (1.614)	0.005 (0.007)	0.005 (0.005)	1.63 (1.623)	1.6 (1.578)

*N is the number of peaks.

Table 5.6. Descriptive Statistics and Normality of Leg Gap Data using method 3 (based on calibrated data)

Type	*N**	Leg Gap (cm)					Skew	Kurtosis	Normal *
		Mean	SD	IQR	Max	Min			
Subject #1									
Normal	37	1.896	0.397	0.433	2.84	1.26	0.745	3.007	Y
Fast	38	1.362	0.398	0.391	2.365	0.861	1.298	3.765	N
Slow	48	1.749	0.475	0.625	3	0.793	0.246	3.09	Y
AntalgicR	37	1.274	0.253	0.303	1.697	0.793	-0.23	2.358	Y
AntalgicL	40	1.995	0.353	0.494	3.079	1.397	0.538	3.689	Y
Subject #2									
Normal	44	2.303	0.256	0.199	3.158	1.57	0.984	6.862	N
Fast	38	2.425	0.381	0.49	3.158	1.697	0.329	2.344	Y
Slow	44	2.282	0.256	0.351	2.947	1.796	0.901	3.207	N
AntalgicR	42	1.574	0.349	0.401	2.683	0.869	0.984	4.576	N
AntalgicL	46	1.996	0.372	0.262	3.158	1.141	0.303	4.344	N
Subject #3									
Normal	52	1.677	0.413	0.545	2.619	0.917	0.44	2.496	Y
Fast	41	1.531	0.446	0.406	3.475	0.932	2.229	10.08	N
Slow	53	1.891	0.445	0.527	3.475	1.11	1.016	4.823	Y
AntalgicR	50	1.525	0.315	0.368	2.523	0.864	0.885	4.214	N
AntalgicL	49	1.735	0.347	0.428	3.079	1.153	1.099	5.819	Y
Subject #4									
Normal	38	1.861	0.348	0.478	2.893	1.199	0.741	3.522	Y
Fast	32	2.841	0.399	0.493	3.953	2.126	0.28	3.374	Y
Slow	34	2.483	0.342	0.409	3.236	1.956	0.645	2.682	Y
AntalgicR	36	3.099	0.537	0.969	3.953	2.195	0.139	1.866	Y
AntalgicL	41	4.054	0.538	0.635	5.273	2.523	0.094	3.914	N

*N is the number of peaks.

Like cadence data, variability in leg gap was measured using maximum (max), minimum (min), interquartile range (IQR), and standard deviation (SD) of leg gap values captured in mid-stance. Skewness and kurtosis of each group of data (subject, stride type) over multiple experiments were also measured to understand deviations from normality of distribution.

Nine of 20 groups failed the Lilliefors test (Table 5.4). Therefore, as mentioned in the previous chapter, subsequent statistical tests for the leg gap did not assume a normal distribution. Out of 20 groups of data, eight (40%) were highly skewed with absolute values greater than 1. Seven (35%) were moderately skewed with absolute values between 0.5 and 1, and the remaining five (25%) distributions were approximately symmetric with values ranging between −0.5 and 0.5 [73]. Only one distribution (corresponding to fast stride for Subject #1 in Table 5.5) was positively skewed. Nineteen distributions (95%) were negatively skewed, indicating that the bulk of the leg gaps were at the mean or larger than the mean. In a majority (89%) of these distributions, the mean was less than the median, a characteristic which is likely but not guaranteed of left skewed distributions. Kurtosis values indicated that a majority of the twenty sample distributions (80%) were more peaked than the normal distribution, indicating that outliers were not as likely among these data groups. Similar trends were shown in data evaluated from leg gap when calculated from empirical calibration data, as illustrated in Table 5.6.

The Kruskal–Wallis test by ranks was used to compare the medians of leg gap associated with abnormal strides (fast, slow) and irregular strides (right antalgic, left antalgic) to the medians of leg gap for normal strides for each individual. Results are summarized in Table 5.7 for all three methods of calculating leg gap. In pairwise comparisons between an abnormal or irregular stride and normal stride for a particular subject, 41 of 60 (68%) shows $p < 0.05$ which means that the null hypothesis was rejected. In other words, the two strides were deemed significantly different in 68% of cases. Comparing all five strides for each subject at once also revealed significant differences among the strides for each of the four subjects (Table 5.7, very right column).

Table 5.7. Comparison of Abnormal and Irregular Strides to Normal Gait
(Kruskal-Wallis Test by ranks of the Null Hypothesis)

		Type of Stride				
		Fast	Slow	Right Antalgic	Left Antalgic	All
Subject	Method	Test Statistic (p-value)				
1	1	*H(1)* = 27.53 (*p* = 0.000***)	*H(1)* = 1.93 (*p* = 0.165)	*H(1)* = 40.08 (*p* = 0.000***)	*H(1)* = 0.34 (*p* = 0.557)	*H(4)* = 71.46 (*p* = 0.000***)
	2	*H(1)* = 27.59 (*p* = 0.000***)	*H(1)* = 1.93 (*p*= 0.165)	*H(1)* = 40.01 (*p* = 0.000***)	*H(1)* = 2.11 (*p* = 0.146)	*H(1)* = 78.14 (*p* = 0.000***)
	3	H(1) = 27.69 (*p* = 0.000***)	*H(1) = 1.91* (*p = 0.167*)	*H(1) = 40.07* (*p* = 0.000***)	*H(1) = 0.1476* (*p = 0.1476*)	*H(4) = 78.09* (*p* = 0.000***)
2	1	*H(1)* = 1.71 (*p* = 0.190)	*H(1)* = 1.42 (*p* = 0.233)	*H(1)* = 51.48 (*p* = 0.000***)	*H(1)* = 26.49 (*p* = 0.000***)	*H(4)* = 100.52 (*p* = 0.000***)
	2	*H(1)* = 1.84 (*p* = 0.176)	*H(1)* = 1.27 (*p* = 0.259)	*H(1)* = 51.52 (*p* = 0.000***)	*H(1)* = 26.06 (*p* = 0.000***)	*H(1)* = 100.1 (*p* = 0.000***)
	3	*H(1) = 1.86* (*p = 0.173*)	*H(1) = 1.25* (*p = 0.263*)	*H(1)* = 51.52 (*p* = 0.000***)	*H(1)* = 25.97 (*p* = 0.000***)	*H(4)* = 100.19 (*p* = 0.000***)
3	1	*H(1)* = 4.19 (*p* = 0.041*)	*H(1)*= 7.02 (*p* = 0.008**)	*H(1)* = 2.83 (*p* = 0.093)	*H(1)* = 1.19 (*p* = 0.276)	*H(4)* = 33.32 (*p* = 0.000***)
	2	*H(1)* = 3.28 (*p* =0.0701)	*H(1)* = 8.39 (*p* = 0.004**)	*H(1)* = 1.87 (*p* = 0.1710)	*H(1)* = 1.85 (*p* = 0.1742)	*H(1)* = 33.32 (*p* = 0.000***)
	3	*H(1)* = 4.65 (*p = 0.031**)	*H(1)*= 6.48 (*p = 0.011**)	*H(1)* = 3.26 (*p = 0.0712*)	*H(1)* = 0.85 (*p = 0.3571*)	*H(4)* = 33.13 (*p* = 0.000***)
4	1	*H(1)* = 44.59 (*p* = 0.000***)	*H(1)* = 34.44 (*p* = 0.000***)	*H(1)* = 50.03 (*p* = 0.000***)	*H(1)* = 58.99 (*p* = 0.000***)	*H(4)* = 135.58 (*p* = 0.000***)
	2	*H(1)* = 44.42 (*p* = 0.000***)	*H(1)* = 34.83 (*p* = 0.000***)	*H(1)* = 50.04 (*p* = 0.000***)	*H(1)* = 58.67 (*p* = 0.000***)	*H(1)* = 135.29 (*p* = 0.000***)
	3	*H(1)* = 44.49 (*p* = 0.000***)	*H(1)* = 34.89 (*p* = 0.000***)	*H(1)* = 49.98 (*p* = 0.000***)	*H(1)* = 58.51 (*p* = 0.000***)	*H(4)* = 135.63 (*p* = 0.000***)

Method 1: Leg gap calculated according to theory using maximum specified sensor sensitivity
Method 2: Leg gap calculated according to theory using minimum specified sensor sensitivity
Method 3: Leg gap calculated according to empirically generated calibration data
* p < 0.05; ** p < 0.01; *** p < 0.001

To evaluate leg gap variability, Levene Test for Equality of Variances was used to evaluate the null hypothesis that two groups (i.e., a normal stride and an abnormal or irregular stride for a particular subject) have equal variances. Results from applying this test to the leg gap data are summarized in Table 5.8. Of the 48 tests comparing variance of abnormal or irregular stride to normal stride, 31 (66%) shows $p < 0.05$ and thus rejected the null hypothesis that the variances were equal. Thus, 66% of strides were accurately identified as abnormal or irregular. This test evaluated against three different sets of data (Methods 1, 2, and 3), similar the Kruskal-Wallis test by ranks.

Table 5.8. Comparison of Abnormal and Irregular Strides to Normal Gait
(Levene Test for Equality of Variances of the Null Hypothesis)

		Type of Stride			
		Fast	Slow	Right Antalgic	Left Antalgic
Subject	Method	Test Statistic (p-value)			
1	1[1]	$F = 14.09$ ($p = 0.0003$***)	$F = 7.28$ ($p = 0.009$**)	$F = 8.04$ ($p = 0.006$**)	$F = 1.19$ ($p = 0.279$)
	2[2]	$F = 12.5730$ ($p = 0.000$***)	$F = 6.8201$ ($p = 0.0107$*)	$F = 6.8907$ ($p = 0.0106$*)	$F = 0.8266$ ($p = 0.3662$)
	3[3]	$F = 0.01714$ ($p = 0.0025$***)	$F = 1.30398$ ($p = 0.2568$***)	$F = 5.88847$ ($p = 0.0177$***)	$F = 0.88135$ ($p = 0.3508$***)
2	1	$F = 4.16$ ($p = 0.048$*)	$F = 0.34$ ($p = 0.562$)	$F = 29.89$ ($p = 0.000$***)	$F = 16.79$ ($p = 0.0001$***)
	2	$F = 4.1055$ ($p = 0.0461$*)	$F = 0.4696$ ($p = 0.4950$)	$F = 28.5124$ ($p = 0.000$***)	$F = 16.7162$ ($p = 0.000$***)
	3	$F = 9.76824$ ($p = 0.048$*)	$F = 0.79423$ ($p = 0.3753$)	$F = 4.13069$ ($p = 0.0453$*)	$F = 3.18581$ ($p = 0.0777$)
3	1	$F = 0.04$ ($p = 0.844$)	$F = 3.92$ ($p = 0.051$)	$F = 1.56$ ($p = 0.214$)	$F = 5.01$ ($p = 0.028$*)
	2	$F = 0.1092$ ($p = 0.7418$)	$F = 3.7961$ ($p = 0.0541$)	$F = 1.9205$ ($p = 0.1689$)	$F = 5.0693$ ($p = 0.0266$*)
	3	$F = 0.52297$ ($p = 0.4714$)	$F = 0.0135$ ($p = 0.9077$)	$F = 5.7088$ ($p = 0.0188$*)	$F = 2.032$ ($p = 0.1572$)
4	1	$F = 29.31$ ($p = 0.000$***)	$F = 22.56$ ($p = 0.000$***)	$F = 33.73$ ($p = 0.000$***)	$F = 59.24$ ($p = 0.000$***)
	2	$F = 28.5321$ ($p = 0.000$***)	$F = 20.7866$ ($p = 0.000$***)	$F = 32.5216$ ($p = 0.000$***)	$F = 59.8071$ ($p = 0.000$***)
	3	$F = 0.46506$ ($p = 0.4976$*)	$F = 0.00473$ ($p = 0.9453$)	$F = 8.99305$ ($p = 0.0037$**)	$F = 2.63634$ ($p = 0.1085$)

Method 1: Leg gap calculated according to theory using maximum specified sensor sensitivity
Method 2: Leg gap calculated according to theory using minimum specified sensor sensitivity
Method 3: Leg gap calculated according to empirically generated calibration data
* $p < 0.05$; ** $p < 0.01$; *** $p < 0.001$

Discussion of these results, and their application to the previously introduced research questions will be further evaluated in Chapter 6, next.

Chapter 6

DISCUSSION

The goal of this study was to evaluate the feasibility of using low-power, compact, high-resolution, analog (linear) Hall-effect sensors to differentiate normal gait from what is abnormal in speed (fast, slow) or irregular in swing (left antalgic, right antalgic). To this end, two gait parameters (cadence and leg gap) were evaluated using a self-contained, single-sensor system to answer two research questions:

6.1. Research Question 1 (RQ1)

Can the wearable system capture cadence with sufficient accuracy to differentiate abnormal and irregular strides from normal strides?

Previous research has indicated that cadence provides a necessary context for evaluating many gait parameters, including that of stride width variability. What constitutes extreme or concerning variability can change with cadence or gait speed of the individual [74]. Thus, an effective wearable gait monitoring system should capture cadence as part of measuring and assessing variability in stride width and related gait parameters. With a temporal resolution of 4 ms in resolving mid-stance events, the wearable Hall-effect sensor system demonstrated here was easily able to differentiate fast and slow strides from normal strides (Table 5.2) because they differed in cadence by 5 steps/minute or more. Comparisons using the Kruskal-Wallis test by ranks for medians successfully detected strides that were not normal from those that were abnormally fast or slow in 100% of cases. Thus, this prototype was able to detect normal from abnormal (fast, slow) gaits through their cadence.

More subtle changes in cadence on the order of 1 step/minute caused by limping (i.e., right antalgic and left antalgic gait) were also captured by the Hall-effect wearable. Thus, while using cadence to detect the difference among fast, slow, and normal strides was fairly trivial because of large differences in the mean cadence for these strides, more nuanced changes in cadence indicated by the similar mean values among normal, right antalgic, and left antalgic strides in Figure 6.1 were also detected with 100% success (Table 5.2).

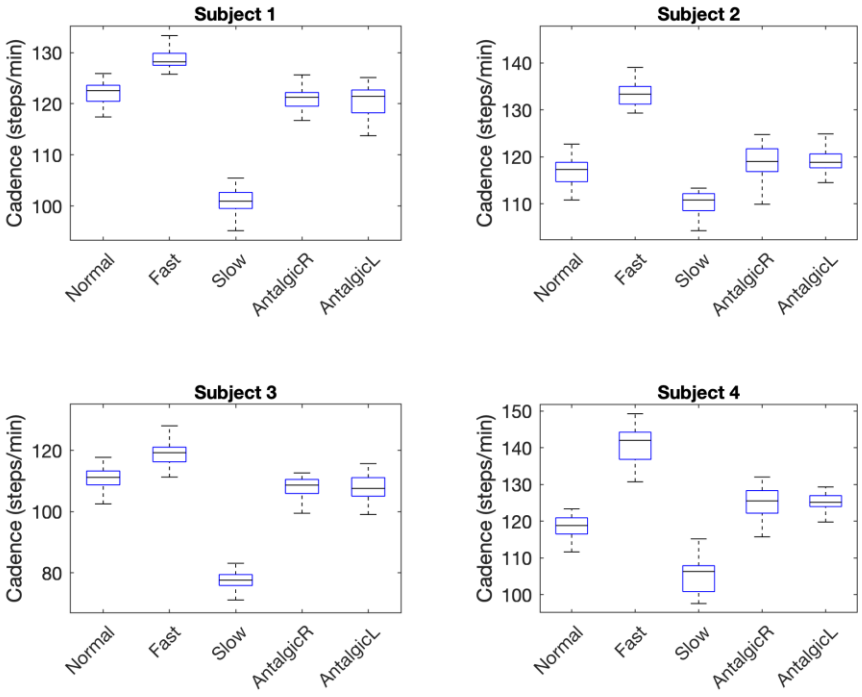

Figure 6.1. Boxplots of Cadence Indicating Differences in Stride Type.

The precision of the Hall-effect wearable allowed for detecting small changes in both mean cadence values and nuances in the distribution of cadence for different stride types. This raises the possibility that with high-resolution systems, cadence might also serve to support characterization of gait and detection of disturbances from normal gait.

Given the evidence of how stable cadence is over an individual's lifetime [75], however, it is not surprising that the variability in cadence across stride types for each individual offered no useful information in differentiating abnormalities or irregularities in stride (Table 5.3). This was demonstrated using the Levene Test (for equality of variances) which determined that abnormal or irregular stride was not equal to that for normal stride in only 19% of the cases.

6.2. Research Question 2 (RQ2)

Does leg gap captured using the wearable system make a sufficient proxy for stride width in terms of differentiating abnormal and irregular strides from normal strides?

This question was evaluated based on the ability of the wearable sensor system to differentiate normal from abnormal or irregular strides. Leg gap (above the knee) is smaller than stride width and subject to smaller variations than stride width. However, it was anticipated that the high precision of the Hall-effect sensors (0.007 cm) in measuring leg gap would compensate for the reduction in leg gap and leg gap variability compared to corresponding stride width parameters (measured at the feet).

The Kruskal-Wallis test by ranks was used to evaluate the medians and rank of leg width of normal stride from that of abnormal or irregular strides. When considering leg gap alone, however, abnormal gait was significantly different from normal gait in only 68% of cases (Table 5.7) and when considering leg gap width variability alone using the Levene Test for equal variances (Table 5.8), 66% of abnormal or irregular stride types were significantly different from normal gait for a particular subject. When considering leg gap and its variability together, abnormal or irregular gait could be differentiated from normal gait in 85% of cases. Thus, leg gap is a promising proxy and alternative to measuring stride gap in terms of differentiating gait types.

Despite the fact that none of the individuals who wore the device during this feasibility study were elderly, the usefulness of leg gap variability in differentiating abnormal and irregular gait from normal gait is promising for detecting unusually small variability and unusually large variability which can indicate balance deficits and other neurological disturbances [19], [22]. In our data, two subjects compensated for simulated balance deficits in right antalgic and left antalgic strides (i.e., limps) via decreased leg gap variability and two compensated with increased leg gap variability. These differences are indicated in the boxplots of Figure 6.2 where the interquartile range (i.e., the height of the box) is higher in Subjects 1 and 2 for antalgic vs. normal strides whereas for Subjects 3 and 4, the interquartile range is smaller for antalgic strides vs. normal strides.

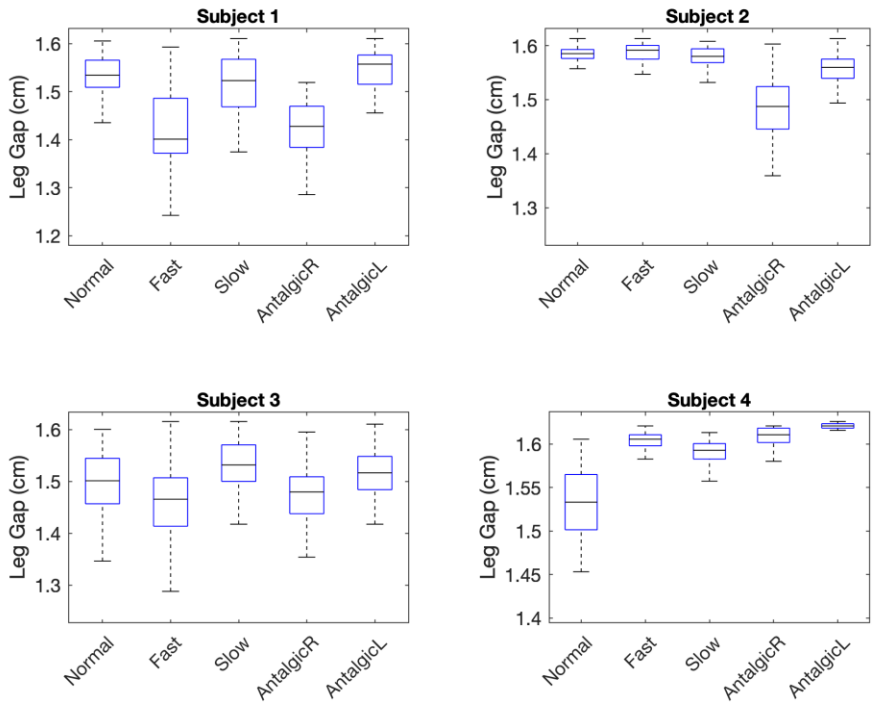

Figure 6.2. Boxplots indicating Leg Gap Variability for Four Subjects.

6.3. Benchmarking—Comparison to Existing Wearables

The feasibility of the leg-mounted Hall-effect wearable has been demonstrated for differentiating two types of abnormal gait (fast, slow) and two types of irregular gait (right antalgic, left antalgic) from normal gait. Such functionality is similar to other efforts (Table 1.3) which have successfully distinguished normal gait from that experienced by individuals recovering from knee surgery [27], suffering from Parkinson's disease [6], [8], [34] or cerebrospinal meningitis [44], living with diabetes [48], or exercising simulated gait disturbances including obstacle courses [58] and toe joint restrictions [45]. Beyond this basic functionality, however, the Hall-effect approach offers some advantages and poses some disadvantages compared to existing systems.

Pros: The Hall-effect wearable offers high precision (on the order of tenths of millimeters) in detecting leg gap compared to existing systems which offer precisions on the order of cm in detecting stride width [43], [51]. While such precision is necessary to monitoring leg gap which is inherently less variable than

stride width as measured at the feet, this increased precision nevertheless offers a greater potential to detect nuances in stride and stance variability. Further, this system offers the possibility of monitoring disturbances in gait with a single sensor at a single location on the body, whereas many existing systems (Tables 2.1 and Table 2.2) use multiple types of sensors or multiple sensors worn on several parts of the body to perform this function. The Hall-effect approach also offers some advantages in power consumption, lifetime, cost, and size. The Hall-effect sensor used in this work consumes appreciable power (on the order of 25 mW) because it requires a continuous supply current of approximately 10 mA to operate properly. However, Allegro Microsystems has replaced the 1302 with sensors from the 139X series [76] which offer a sleep mode that consumes only 0.08 mW, thereby offering significantly reduced overall power consumption in an application such as gait monitoring where the sensor need only be awake for a small fraction of time (i.e., when an individual is walking). Furthermore, unlike accelerometers, bend sensors, gyros, and similar sensors, the Hall-effect sensor has no moving parts, thus offering an increased lifetime among wearable gait sensors. The small footprint of these sensors also allows for comfortable and realistic packaging for everyday monitoring and by nature, magnetic sensor technology allow for non-invasive continuous monitoring, which is paramount for continuous monitoring devices. Mounting along the thigh rather than the foot also decreases the mechanical stresses to which the sensor is subject, further increasing its lifetime. Finally, linear Hall-effect sensors are inexpensive (less than two dollars) compared to other sensors and smaller in size (Table 6.1). Since leg gap can be estimated using a simple look-up table, as demonstrated in Method 3 using empirical data, the overhead (cost, power, size), involved in extracting useful information from a Hall-effect wearable is also much lower than most other sensors used in gait monitoring wearables.

Table 6.1. Typical Constraints of Sensors Used in Wearable Gait Monitors.

Parameter (Sensor Type)	Example	Power [mW] [1]	Cost [USD] [4]	Size [cm] [5]	Weight [g]
Bending/Vibration (PVDF Strips)	TE Connectivity LDT0 [77] used in [34]	NA	$2.69	2.5 × 1.3	NA
Angular rate, orientation (gyroscope)	Analog Devices ADXRS290 similar to ADXRS150 [78] used in [34]	39 (0.4) [2]	$16.06	0.6 × 0.4	NA
Acceleration, angular rate, orientation (IMU)	XSens MTi-1 [79]	45	$139	1.2 × 1.2	0.66
Distance (Hall-effect)	Allegro 139X [69] replacement for sensors used here	9.6 (0.08) [2]	$1.20	0.8 × 0.3	0.014
Distance (Infrared IR)	Sharp GP2YOA41SKOF [80] used in [65]	60	$9.93	4.4 × 1.9	3.5
Distance (Ultrasonic)	URM07 [81]	25 (0.07) [2]	$5.59	2.7 × 2.7	4.2
Force/Pressure (Force-Sensitive Resistor)	FSR-400 [82] used in [34]	2.5 [3]	$4.40	4.0 × 4.0	NA
Linear Acceleration (accelerometer)	Analog Devices ADXL202E [83] used in [34]	3.0	$19.72	0.7 × 0.7	5
Object Presence (electric field sensors)	Motorola MC33794DH [79] used in [34]	98	$24 (est)	1.6 × 1.1	NA

[1] Power consumption provided at typical supply voltages (as specified in datasheet). [2] In measurement (sleep) or measurement (non-actuated) mode at typical supply voltage. [3] Based on 10 k measurement resistance when bent and a basic measurement circuit. [4] Cost estimated at quantities of 100 units. [5] Thickness was either not specified or is small compared to remaining two dimensions; NA: not available.

Cons: Compared to the wealth of spatiotemporal information offered by accelerometers, gyros, and IMUs, the Hall-effect approach offers limited data. Its range is insufficient for monitoring stride length and other gait parameters that extend larger than 5 cm and temporal patterns of information are restricted to at or near mid-stance peaks. The leg wearable is also only suited to monitoring gait within an individual's walking patterns and not across individuals. Comparing data between individuals is subject to too much variation in mounting location and other compliance related issues. These issues are minimized when sensors are integrated into the more rigid footprint provided by the shoe. However, one can easily imagine a highly inobtrusive Hall-effect sensor or sensors integrated into clothing which provide a low-overhead indicator of generalized gait disturbance and flags the potential need to monitor gait more comprehensively with the assistance of clinical or wearable systems that are designed to do so. Alternatively, these Hall-effect sensor systems can be paired with higher overhead wearables using

accelerometers or similar conventional sensors mounted in the shoe; in this scenario, power consumption of the paired wearables can be minimized by using the Hall-effect sensor to "wake-up" wearables in the shoe when abnormalities or irregularities in gait are detected.

6.4. Future Work

The work presented here has focused on studying the feasibility of using Hall-effect sensors to identify gait disturbances. Statistical analyses suggest that leg gap, variability in leg gap, and cadence offer significant information for differentiating abnormal and irregular gait from normal gait. Future work should capitalize on the results of this work to explore efficient algorithms for recognizing gait disturbances based on cadence and leg gap data provided by these wearables. Similarly, future work could improve upon the manual pre-processing nature of this data by creating more efficient algorithms to identify additional gait phases, including that of mid-stance peaks as used in this research. Time series analyses of the entire stride (rather than only the mid-stance peak) should also be considered in future efforts to explore the full functionality of the Hall-effect wearable in supporting everyday gait monitoring. In a step further, future work of this research should also include study of gait typical to everyday lifestyle such as turns, stairs, running, jogging etc. Concurrently, we expect that future work will seek to miniaturize the wearable system such that it fully takes advantage of the small size and lower power sleep modes of the A139X series of Hall-effect sensors. Finally, the suitability of pairing a Hall-effect sensor wearable with a more comprehensive gait monitoring wearable will also be a topic of future research in this area.

Chapter 7

CONCLUSION

The feasibility of using linear analog Hall-effect sensors in a wearable system for monitoring spatiotemporal gait parameters associated with cadence and leg gap has been evaluated through two research questions. The measurement of gait parameters such as cadence and stride width support the important study of various health problems, including disease, disorder, physical and neurological impairments, and recovery and rehabilitation. Results show that leg gap and leg gap variability (as a proxy for stride width) and cadence data collected from these sensors can successfully detect disturbances in gait within individuals. For the controlled experiments used in this feasibility study, the temporal parameter of cadence offered 100% accuracy in differentiating abnormal or irregular strides from normal strides (i.e., gait disturbance). 68% accuracy in identifying gait disturbance was demonstrated when using leg gap alone, 66% accuracy when using leg gap variability alone, and 85% accuracy when using both in combination. The Hall-effect systems can be used alone to indicate when gait starts to exhibit abnormal or irregular trends, or it may be used as a supplement to traditional, clinical systems to track gait continuously in everyday life in order to confirm or deny clinical findings. The results demonstrated in this prototype are promising in providing a means to monitor gait both as a supplement to more complex and expensive clinical systems or as an alternative to such systems in rural or underserved areas.

REFERENCES

[1] Chakravarthy, Y.K., "Design and Development of an Indigenous and Intelligent Transfemoral Prosthetic Leg," PhD Thesis, Koneru Lakshmaiah Education Foundation, 2018. Accessed: Dec. 30, 2020. [Online]. Available: http://hdl.handle.net/10603/213619

[2] Y. Moon, J. Sung, R. An, M. E. Hernandez, and J. J. Sosnoff, "Gait variability in people with neurological disorders: A systematic review and meta-analysis," *Hum. Mov. Sci.*, vol. 47, pp. 197–208, Jun. 2016, doi: 10.1016/j.humov.2016.03.010.

[3] B. Galna, S. Lord, and L. Rochester, "Is gait variability reliable in older adults and Parkinson's disease? Towards an optimal testing protocol," *Gait Posture*, vol. 37, no. 4, pp. 580–585, Apr. 2013, doi: 10.1016/j.gaitpost.2012.09.025.

[4] P. Esser, H. Dawes, J. Collett, and K. Howells, "Insights into gait disorders: Walking variability using phase plot analysis, Parkinson's disease," *Gait Posture*, vol. 38, no. 4, pp. 648–652, Sep. 2013, doi: 10.1016/j.gaitpost.2013.02.016.

[5] "Parkinson's disease - Symptoms and causes," *Mayo Clinic*. https://www.mayoclinic.org/diseases-conditions/parkinsons-disease/symptoms-causes/syc-20376055 (accessed Sep. 15, 2021).

[6] M. D. Djuric-Jovicic, N. S. Jovicic, S. M. Radovanovic, I. D. Stankovic, M. B. Popovic, and V. S. Kostic, "Automatic Identification and Classification of Freezing of Gait Episodes in Parkinson's Disease Patients," *IEEE Trans. Neural Syst. Rehabil. Eng.*, vol. 22, no. 3, pp. 685–694, May 2014, doi: 10.1109/TNSRE.2013.2287241.

[7] J. M. Hausdorff, M. E. Cudkowicz, R. Firtion, J. Y. Wei, and A. L. Goldberger, "Gait variability and basal ganglia disorders: Stride-to-stride variations of gait cycle timing in parkinson's disease and Huntington's disease," *Mov. Disord.*, vol. 13, no. 3, pp. 428–437, May 1998, doi: 10.1002/mds.870130310.

[8] A. Salarian *et al.*, "Gait Assessment in Parkinson's Disease: Toward an Ambulatory System for Long-Term Monitoring," *IEEE Trans. Biomed. Eng.*, vol. 51, no. 8, pp. 1434–1443, Aug. 2004, doi: 10.1109/TBME.2004.827933.

[9] J. Jankovic, "Parkinson's disease: clinical features and diagnosis," *J. Neurol. Neurosurg. Psychiatry*, vol. 79, no. 4, pp. 368–376, Apr. 2008, doi: 10.1136/jnnp.2007.131045.

[10] C.-N. Lee, V. H. Fong, Y.-T. Chu, L. Cheng, H.-W. Chuang, and C.-Y. Lo, "A Wearable Device Of Gait Tracking For Parkinson'S Disease Patients," in *2018 International Conference on Machine Learning and Cybernetics (ICMLC)*, Chengdu, Jul. 2018, pp. 462–466. doi: 10.1109/ICMLC.2018.8527011.

[11] S. T. O'Keeffe, H. Kazeem, R. M. Philpott, J. R. Playfer, M. Gosney, and M. Lye, "Gait disturbance in Alzheimer's disease: a clinical study," *Age Ageing*, vol. 25, no. 4, pp. 313–316, Jul. 1996, doi: 10.1093/ageing/25.4.313.

[12] L. Z. Gras, S. F. Kanaan, J. M. McDowd, Y. M. Colgrove, J. Burns, and P. S. Pohl, "Balance and Gait of Adults With Very Mild Alzheimer Disease:," *J. Geriatr. Phys. Ther.*, vol. 38, no. 1, pp. 1–7, 2015, doi: 10.1519/JPT.0000000000000020.

[13] P. L. Sheridan, J. Solomont, N. Kowall, and J. M. Hausdorff, "Influence of Executive Function on Locomotor Function: Divided Attention Increases Gait Variability in Alzheimer's Disease," *J. Am. Geriatr. Soc.*, vol. 51, no. 11, pp. 1633–1637, 2003, doi: 10.1046/j.1532-5415.2003.51516.x.

[14] I. Mileti, J. Taborri, S. Rossi, M. Petrarca, F. Patane, and P. Cappa, "Evaluation of the effects on stride-to-stride variability and gait asymmetry in children with Cerebral Palsy wearing the WAKE-up ankle module," in *2016 IEEE International Symposium on Medical Measurements and Applications (MeMeA)*, Benevento, Italy, May 2016, pp. 1–6. doi: 10.1109/MeMeA.2016.7533748.

[15] J. M. Hausdorff *et al.*, "Altered fractal dynamics of gait: reduced stride-interval correlations with aging and Huntington's disease," *J. Appl. Physiol.*, vol. 82, no. 1, pp. 262–269, Jan. 1997, doi: 10.1152/jappl.1997.82.1.262.

[16] B. M. Meyer *et al.*, "Wearables and Deep Learning Classify Fall Risk From Gait in Multiple Sclerosis," *IEEE J. Biomed. Health Inform.*, vol. 25, no. 5, pp. 1824–1831, May 2021, doi: 10.1109/JBHI.2020.3025049.

[17] M. R. Lemke, T. Wendorff, B. Mieth, K. Buhl, and M. Linnemann, "Spatiotemporal gait patterns during over ground locomotion in major depression compared with healthy controls," *J. Psychiatr. Res.*, vol. 34, no. 4–5, pp. 277–283, Jul. 2000, doi: 10.1016/S0022-3956(00)00017-0.

[18] J. M. Hausdorff, C.-K. Peng, A. L. Goldberger, and A. L. Stoll, "Gait unsteadiness and fall risk in two affective disorders: a preliminary study," *BMC Psychiatry*, vol. 4, no. 1, p. 39, Nov. 2004, doi: 10.1186/1471-244X-4-39.

[19] J. S. Brach, S. Studenski, S. Perera, J. M. VanSwearingen, and A. B. Newman, "Stance time and step width variability have unique contributing impairments in older persons," *Gait Posture*, vol. 27, no. 3, pp. 431–439, Apr. 2008, doi: 10.1016/j.gaitpost.2007.05.016.

[20] "Fast Facts of Common Eye Disorders | CDC," Jun. 09, 2020. https://www.cdc.gov/visionhealth/basics/ced/fastfacts.htm (accessed Aug. 31, 2021).

[21] A. H. Snijders, B. P. van de Warrenburg, N. Giladi, and B. R. Bloem, "Neurological gait disorders in elderly people: clinical approach and classification," *Lancet Neurol.*, vol. 6, no. 1, pp. 63–74, Jan. 2007, doi: 10.1016/S1474-4422(06)70678-0.

[22] J. M. Hausdorff, D. A. Rios, and H. K. Edelberg, "Gait variability and fall risk in community-living older adults: A 1-year prospective study," *Arch. Phys. Med. Rehabil.*, vol. 82, no. 8, pp. 1050–1056, Aug. 2001, doi: 10.1053/apmr.2001.24893.

[23] S. L. Vaught, "Gait, Balance, and Fall Prevention," *Ochsner J.*, vol. 3, no. 2, pp. 94–97, Apr. 2001.

[24] J. Verghese, R. B. Lipton, C. B. Hall, G. Kuslansky, M. J. Katz, and H. Buschke, "Abnormality of Gait as a Predictor of Non-Alzheimer's Dementia," *N. Engl. J. Med.*, vol. 347, no. 22, pp. 1761–1768, Nov. 2002, doi: 10.1056/NEJMoa020441.

[25] J. M. VanSwearingen, K. A. Paschal, P. Bonino, and T. W. Chen, "Assessing recurrent fall risk of community-dwelling, frail older veterans using specific tests of mobility and the physical performance test of function," *J. Gerontol. A. Biol. Sci. Med. Sci.*, vol. 53, no. 6, pp. M457-464, Nov. 1998, doi: 10.1093/gerona/53a.6.m457.

[26] J. R. Yong, A. Silder, K. L. Montgomery, M. Fredericson, and S. L. Delp, "Acute changes in foot strike pattern and cadence affect running parameters associated with tibial stress fractures," *J. Biomech.*, vol. 76, pp. 1–7, Jul. 2018, doi: 10.1016/j.jbiomech.2018.05.017.

[27] K. Makino, M. Nakamura, H. Omori, and H. Terada, "Gait analysis using Gravity-Center Fluctuation of the sole at walking based on Self-Organizing Map," in *2015 IEEE 24th International Symposium on Industrial Electronics (ISIE)*, Buzios, Rio de Janeiro, Brazil, Jun. 2015, pp. 900–905. doi: 10.1109/ISIE.2015.7281590.

[28] W. Tao, T. Liu, R. Zheng, and H. Feng, "Gait Analysis Using Wearable Sensors," *Sensors*, vol. 12, no. 2, pp. 2255–2283, Feb. 2012, doi: 10.3390/s120202255.

[29] X. Wu, X. Chen, Y. Duan, S. Xu, N. Cheng, and N. An, "A study on gait-based Parkinson's disease detection using a force sensitive platform," in *2017 IEEE International Conference on Bioinformatics and Biomedicine (BIBM)*, Kansas City, MO, Nov. 2017, pp. 2330–2332. doi: 10.1109/BIBM.2017.8218048.

[30] A. Muro-de-la-Herran, B. Garcia-Zapirain, and A. Mendez-Zorrilla, "Gait Analysis Methods: An Overview of Wearable and Non-Wearable Systems, Highlighting Clinical Applications," *Sensors*, vol. 14, no. 2, pp. 3362–3394, Feb. 2014, doi: 10.3390/s140203362.

[31] P. Bonato *et al.*, "IEEE EMBS Technical Committee on Wearable Biomedical Sensors & Systems: Position Paper," in *International Workshop on Wearable and Implantable Body Sensor Networks (BSN'06)*, Cambridge, MA, USA, 2006, pp. 212–214. doi: 10.1109/BSN.2006.28.

[32] M. M. Rodgers, V. M. Pai, and R. S. Conroy, "Recent Advances in Wearable Sensors for Health Monitoring," *IEEE Sens. J.*, vol. 15, no. 6, pp. 3119–3126, Jun. 2015, doi: 10.1109/JSEN.2014.2357257.

[33] S. Majumder, T. Mondal, and M. Deen, "Wearable Sensors for Remote Health Monitoring," *Sensors*, vol. 17, no. 12, p. 130, Jan. 2017, doi: 10.3390/s17010130.

[34] S. Bamberg, A. Y. Benbasat, D. M. Scarborough, D. E. Krebs, and J. A. Paradiso, "Gait Analysis Using a Shoe-Integrated Wireless Sensor System," *IEEE Trans. Inf. Technol. Biomed.*, vol. 12, no. 4, pp. 413–423, Jul. 2008, doi: 10.1109/TITB.2007.899493.

[35] A. Jo, B. D. Coronel, C. E. Coakes, and A. G. Mainous, "Is There a Benefit to Patients Using Wearable Devices Such as Fitbit or Health Apps on Mobiles? A Systematic Review," *Am. J. Med.*, vol. 132, no. 12, pp. 1394-1400.e1, Dec. 2019, doi: 10.1016/j.amjmed.2019.06.018.

[36] "Wearable Technology Market Size | Industry Report, 2020-2027." https://www.grandviewresearch.com/industry-analysis/wearable-technology-market (accessed Sep. 15, 2021).

[37] "Harnessing wearable device data to improve state-level real-time surveillance of influenza-like illness in the USA: a population-based study - The Lancet Digital Health." https://www.thelancet.com/journals/landig/article/PIIS2589-7500(19)30222-5/fulltext (accessed Dec. 30, 2020).

[38] D. Brown, "'It saved my life': Apple Watch, Fitbit are notifying users of medical emergencies," *USA TODAY*. https://www.usatoday.com/story/tech/2019/02/20/can-smartwatches-literally-save-lives-some-users-say-yes/2646598002/ (accessed Dec. 30, 2020).

[39] A. Oldham, K. M. Stepien, and C. J. Hendriksz, "Potential benefits of Fitbit device in managing a patient with mucopolysaccharidosis," *Mol. Genet. Metab.*, vol. 126, no. 2, p. S111, Feb. 2019, doi: 10.1016/j.ymgme.2018.12.281.

[40] A. M. Abrantes, C. E. Blevins, C. L. Battle, J. P. Read, A. L. Gordon, and M. D. Stein, "Developing a Fitbit-supported lifestyle physical activity intervention for depressed alcohol dependent women," *J. Subst. Abuse Treat.*, vol. 80, pp. 88–97, Sep. 2017, doi: 10.1016/j.jsat.2017.07.006.

[41] "IDC - Wearable Devices Market Share," *IDC: The premier global market intelligence company*. https://www.idc.com/promo/wearablevendor (accessed Dec. 30, 2020).

[42] D. Kobsar *et al.*, "Wearable Inertial Sensors for Gait Analysis in Adults with Osteoarthritis—A Scoping Review," *Sensors*, vol. 20, no. 24, Art. no. 24, Jan. 2020, doi: 10.3390/s20247143.

[43] M. Hao, K. Chen, and C. Fu, "Smoother-Based 3-D Foot Trajectory Estimation Using Inertial Sensors," *IEEE Trans. Biomed. Eng.*, vol. 66, no. 12, pp. 3534–3542, Dec. 2019, doi: 10.1109/TBME.2019.2907322.

[44] T.-H. Yu and C.-C. Wu, "An Accelerometer Based Gait Analysis System to Detect Gait Abnormalities in Cerebralspinal Meningitis Patients," in *2019 International Conference on Machine Learning and Cybernetics (ICMLC)*, Kobe, Japan, Jul. 2019, pp. 1–5. doi: 10.1109/ICMLC48188.2019.8949256.

[45] G. Li, T. Liu, and J. Yi, "Wearable Sensor System for Detecting Gait Parameters of Abnormal Gaits: A Feasibility Study," *IEEE Sens. J.*, vol. 18, no. 10, pp. 4234–4241, May 2018, doi: 10.1109/JSEN.2018.2814994.

[46] W.-L. Hsi, H.-M. Chai, and J.-S. Lai, "Comparison of Pressure and Time Parameters in Evaluating Diabetic Footwear:," *Am. J. Phys. Med. Rehabil.*, vol. 81, no. 11, pp. 822–829, Nov. 2002, doi: 10.1097/00002060-200211000-00004.

[47] O. Bai, R. Atri, J. S. Marquez, and D.-Y. Fei, "Characterization of lower limb activity during gait using wearable, multi-channel surface EMG and IMU sensors," p. 4, 2017.

[48] M. Munoz-Organero, J. Parker, L. Powell, R. Davies, and S. Mawson, "Sensor Optimization in Smart Insoles for Post-Stroke Gait Asymmetries Using Total Variation and L 1 Distances," *IEEE Sens. J.*, vol. 17, no. 10, pp. 3142–3151, May 2017, doi: 10.1109/JSEN.2017.2686641.

[49] P. Duong and Y. Suh, "Foot Pose Estimation Using an Inertial Sensor Unit and Two Distance Sensors," *Sensors*, vol. 15, no. 7, pp. 15888–15902, Jul. 2015, doi: 10.3390/s150715888.

[50] I. H. López-Nava, "Estimation of temporal gait parameters using Bayesian models on acceleration signals," *Comput. Methods Biomech. Biomed. Engin.*, p. 9.

[51] D. Weenk, D. Roetenberg, B. J. F. van Beijnum, H. J. Hermens, and P. H. Veltink, "Ambulatory Estimation of Relative Foot Positions by Fusing Ultrasound and Inertial Sensor Data," *IEEE Trans. Neural Syst. Rehabil. Eng.*, vol. 23, no. 5, pp. 817–826, Sep. 2015, doi: 10.1109/TNSRE.2014.2357686.

[52] D. Novak, M. Goršič, J. Podobnik, and M. Munih, "Toward Real-Time Automated Detection of Turns during Gait Using Wearable Inertial Measurement Units," *Sensors*, vol. 14, no. 10, pp. 18800–18822, Oct. 2014, doi: 10.3390/s141018800.

[53] J. Taborri, S. Rossi, E. Palermo, F. Patanè, and P. Cappa, "A Novel HMM Distributed Classifier for the Detection of Gait Phases by Means of a Wearable Inertial Sensor Network," *Sensors*, vol. 14, no. 9, Art. no. 9, Sep. 2014, doi: 10.3390/s140916212.

[54] T. N. Hung and Y. S. Suh, "Inertial Sensor-Based Two Feet Motion Tracking for Gait Analysis," *Sensors*, vol. 13, no. 5, Art. no. 5, May 2013, doi: 10.3390/s130505614.

[55] A. Salarian, P. R. Burkhard, F. J. G. Vingerhoets, B. M. Jolles, and K. Aminian, "A Novel Approach to Reducing Number of Sensing Units for Wearable Gait Analysis Systems," *IEEE Trans. Biomed. Eng.*, vol. 60, no. 1, pp. 72–77, Jan. 2013, doi: 10.1109/TBME.2012.2223465.

[56] T. Sayeed, A. Sama, A. Catala, and J. Cabestany, "Comparative and adaptation of step detection and step length estimators to a lateral belt worn accelerometer," in *2013 IEEE 15th International Conference on e-Health Networking, Applications and Services (Healthcom 2013)*, Lisbon, Portugal, Oct. 2013, pp. 105–109. doi: 10.1109/HealthCom.2013.6720648.

[57] T. Liu, Y. Inoue, and K. Shibata, "A Wearable Ground Reaction Force Sensor System and Its Application to the Measurement of Extrinsic Gait Variability," *Sensors*, vol. 10, no. 11, Art. no. 11, Nov. 2010, doi: 10.3390/s101110240.

[58] T. Liu, Y. Inoue, and K. Shibata, "Development of a wearable sensor system for quantitative gait analysis," *Measurement*, vol. 42, no. 7, pp. 978–988, Aug. 2009, doi: 10.1016/j.measurement.2009.02.002.

[59] H. M. Schepers, H. F. J. M. Koopman, and P. H. Veltink, "Ambulatory Assessment of Ankle and Foot Dynamics," *IEEE Trans. Biomed. Eng.*, vol. 54, no. 5, pp. 895–902, May 2007, doi: 10.1109/TBME.2006.889769.

[60] J. Petrofsky, S. Lee, and S. Bweir, "Gait characteristics in people with type 2 diabetes mellitus," *Eur. J. Appl. Physiol.*, vol. 93, no. 5–6, pp. 640–647, Mar. 2005, doi: 10.1007/s00421-004-1246-7.

[61] M. A. Razian and M. G. Pepper, "Design, development, and characteristics of an in-shoe triaxial pressure measurement transducer utilizing a single element of piezoelectric copolymer film," *IEEE Trans. Neural Syst. Rehabil. Eng.*, vol. 11, no. 3, pp. 288–293, Sep. 2003, doi: 10.1109/TNSRE.2003.818185.

[62] K. Aminian, B. Najafi, C. Büla, P.-F. Leyvraz, and Ph. Robert, "Spatio-temporal parameters of gait measured by an ambulatory system using miniature gyroscopes," *J. Biomech.*, vol. 35, no. 5, pp. 689–699, May 2002, doi: 10.1016/S0021-9290(02)00008-8.

[63] R. B. Huitema, A. L. Hof, and K. Postema, "Ultrasonic motion analysis system—measurement of temporal and spatial gait parameters," *J. Biomech.*, vol. 35, no. 6, pp. 837–842, Jun. 2002, doi: 10.1016/S0021-9290(02)00032-5.

[64] S. Miyazaki, "Long-term unrestrained measurement of stride length and walking velocity utilizing a piezoelectric gyroscope," *IEEE Trans. Biomed. Eng.*, vol. 44, no. 8, pp. 753–759, Aug. 1997, doi: 10.1109/10.605434.

[65] A. Arami, N. Vida Martins, and K. Aminian, "Locally Linear Neuro-Fuzzy Estimate of the Prosthetic Knee Angle and Its Validation in a Robotic Simulator," *IEEE Sens. J.*, vol. 15, no. 11, pp. 6271–6278, Nov. 2015, doi: 10.1109/JSEN.2015.2451361.

[66] T. D. Laovoravit, N. A. Stomberg, and B. L. Lam, "MagneForce: Validation of a Modular Tri-Axial Force Sensor for Gait Analysis," Apr. 27, 2017.

[67] "K&J Magnetics - Neodymium Magnet Information." https://www.kjmagnetics.com/neomaginfo.asp (accessed Sep. 15, 2021).

[68] "K&J Magnetics: RX054-N52." https://www.kjmagnetics.com/proddetail.asp?prod=RX054-N52 (accessed Sep. 15, 2021).
[69] "Allegro MicroSystems - A1301 and A1302: Continuous-Time Ratiometric Linear Hall Effect Sensor ICs." https://www.allegromicro.com/en/products/discontinued-product-archive/a1301-2 (accessed Jan. 21, 2021).
[70] W. H. Kruskal and W. A. Wallis, "Use of Ranks in One-Criterion Variance Analysis," *J. Am. Stat. Assoc.*, vol. 47, no. 260, pp. 583–621, Dec. 1952, doi: 10.1080/01621459.1952.10483441.
[71] I. Olkin and I. Olkin, *Contributions to probability and statistics*. Stanford, Calif.: Stanford, Calif., Stanford University Press, 1960.
[72] H. W. Lilliefors, "On the Kolmogorov-Smirnov Test for Normality with Mean and Variance Unknown," *J. Am. Stat. Assoc.*, vol. 62, no. 318, pp. 399–402, Jun. 1967, doi: 10.1080/01621459.1967.10482916.
[73] M. Bulmer, "Principles of Statistics Dover Publications," *N. Y.*, 1979.
[74] J. S. Brach, J. E. Berlin, J. M. VanSwearingen, A. B. Newman, and S. A. Studenski, "Too much or too little step width variability is associated with a fall history in older persons who walk at or near normal gait speed," *J. NeuroEngineering Rehabil.*, p. 8, 2005.
[75] A. Aboutorabi, M. Arazpour, M. Bahramizadeh, S. W. Hutchins, and R. Fadayevatan, "The effect of aging on gait parameters in able-bodied older subjects: a literature review," *Aging Clin. Exp. Res.*, vol. 28, no. 3, pp. 393–405, Jun. 2016, doi: 10.1007/s40520-015-0420-6.
[76] EETimes, "EETimes - Allegro MicroSystems : Hall-effect sensors consume very little power -," *EETimes*, Mar. 03, 2008. https://www.eetimes.com/allegro-microsystems-hall-effect-sensors-consume-very-little-power/ (accessed Jan. 21, 2021).
[77] "Piezo Film Vibration Sensor/Switch," *TE Connectivity*. https://www.te.com/usa-en/product-CAT-PFS0006.html (accessed Jan. 21, 2021).
[78] "ADXRS290 Datasheet and Product Info | Analog Devices." https://www.analog.com/en/products/adxrs290.html# (accessed Jan. 21, 2021).
[79] "MTI-1-T XSens Technologies BV | Sensors, Transducers | DigiKey." https://www.digikey.com/en/products/detail/xsens-technologies-bv/MTI-1-T/5773873 (accessed Jan. 21, 2021).
[80] "Pololu - Sharp GP2Y0A41SK0F Analog Distance Sensor 4-30cm." https://www.pololu.com/product/2464/specs (accessed Jan. 21, 2021).
[81] "URM07-UART_Ultrasonic_Sensor_SKU__SEN0153-DFRobot." https://wiki.dfrobot.com/URM07-UART_Ultrasonic_Sensor_SKU__SEN0153 (accessed Jan. 21, 2021).
[82] I. E. Inc, "FSR 400." https://www.interlinkelectronics.com/fsr-400 (accessed Jan. 21, 2021).
[83] "ADXL202 Datasheet and Product Info | Analog Devices." https://www.analog.com/en/products/adxl202.html#product-overview (accessed Jan. 21, 2021).